PERIODIC DISTURBANCE ESTIMATION BASED ROBUST CONTROL OF MARINE VEHICLES

A Thesis Submitted to
the Graduate School of
İzmir Institute of Technology
in Partial Fulfillment of the Requirements for the Degree of

MASTER OF SCIENCE

in Electronics and Communication Engineering

by
Deniz KURTOĞLU

July 2020
İZMİR

ACKNOWLEDGMENTS

I would like to express my gratefulness to my advisor Prof. Dr. Enver Tatlıcıoğlu for his endless understanding, support, and priceless guidance throughout my thesis study. I am indebted to him for introducing me to the control of marine vehicles as well.

Furthermore, I would like to use this opportunity to thank Doç. Dr. Barış Bıdıklı and Prof. Dr. Erkan Zergeroğlu for their invaluable suggestion and comments for my work.

I would also give special thanks to Mehmet Onur Cirit for his suggestions and continual encouragement throughout my study. Moreover, I would like to thank Ali Bars Gündüz for his precious help, and to Berna Derya Deniz for helping me draw a figure in my thesis.

My deepest appreciation must go to my mother and my father. Without their support, patience, and belief in me, I could not have succeeded.

ABSTRACT

PERIODIC DISTURBANCE ESTIMATION BASED ROBUST CONTROL OF MARINE VEHICLES

Highly uncertain and complex structures of marine vehicles render the control problem a challenging task. Moreover, the problem becomes much more challenging when the system is exposed to environmental disturbances. This thesis tackles this control problem with an adaptive robust control algorithm which is fused with a periodic disturbance estimation method. The periodic disturbance estimation method inspired from a Fourier series expansion technique is applied for compensation of environmental forces.

In the first part of the thesis, an adaptive full state feedback backstepping controller which is supported with the periodic disturbance estimation method is applied. Stability of the closed–loop system and the convergence of the tracking error are established via Lyapunov based methods. Simulation studies are provided to support the theoretical results and to demonstrate the effectiveness of the proposed method.

In the second part of the thesis, a nonlinear model free observer based adaptive output feedback controller in conjunction with the periodic disturbance estimator is designed. Lyapunov based arguments have been utilized to prove the stability of the closed–loop system, and the convergence of the tracking and observer errors under the closed–loop operation. Performance and viability of the proposed method are demonstrated via numerical simulations.

ÖZET

DENİZ ARAÇLARININ PERİYODİK BOZAN ETKEN KESTİRİMLİ GÜRBÜZ DENETİMİ

Deniz araçlarının son derece belirsiz ve karmaşık yapıları kontrol problemini zor bir görev haline getirmektedir. Ek olarak, sistem çevresel bozan etkenlere maruz kaldığında bu problem daha da zorlaşmaktadır. Bu tez, bu kontrol problemini periyodik bozan etken kestirimi yöntemi ile birleştirilmiş uyarlamalı gürbüz denetim ile ele almaktadır. Çevresel kuvvetlerin telafisi için Fourier serisi açılımı tekniğinden esinlenen periyodik bozan etken kestirimi yöntemi uygulanmıştır.

Tezin ilk bölümünde, periyodik bozan etken kestirimi yöntemi ile desteklenen uyarlamalı tüm durum geri beslemeli geri adımlamalı denetleyici uygulanmıştır. Kapalı döngü sistemin kararlılığı ve takip hatasının yakınsaması Lyapunov temelli yöntemler ile belirlenmiştir. Teorik sonuçları desteklemek ve önerilen yöntemin etkinliğini göstermek için benzetim çalışmaları yapılmıştır.

Tezin ikinci bölümünde, periyodik bozan etken kestirimi yöntemi ile birlikte doğrusal olmayan modelden bağımsız gözlemci tabanlı uyarlamalı çıkış geri beslemeli denetleyici tasarlanmıştır. Sistemin kararlılığını ve kapalı döngü altında takip ve gözlemci hatalarının yakınsamasını kanıtlamak için Lyapunov tabanlı yöntemler kullanılmıştır. Önerilen yöntemin başarımı ve uygulanabilirliği sayısal benzetimlerle gösterilmiştir.

TABLE OF CONTENTS

LIST OF FIGURES

Figure **Page**

LIST OF TABLES

Table **Page**

LIST OF SYMBOLS

$\eta(t)$ ..... Position

$\dot{\eta}(t)$ ..... First time derivative of position

$\ddot{\eta}(t)$ ..... Second time derivative of position

$\nu(t)$ ..... Velocity

$\dot{\nu}(t)$ ..... Time derivative of velocity

R ..... Rotation matrix

M ..... Inertia matrix

C_c ..... Centripetal Coriolis matrix

D ..... Damping matrix

$\tau_d(t)$ ..... Environemental disturbances

$\tau(t)$ ..... Control input torque

$\eta_d(t)$ ..... Desired position

$\dot{\eta}_d(t)$ ..... First time derivative of desired position

$\ddot{\eta}_d(t)$ ..... Second time derivative of desired position

$x(t)$ ..... First entry of position

$y(t)$ ..... Second entry of position

$\psi(t)$ ..... Third entry of position

$\nu_u(t)$ ..... First entry of velocity

$\nu_v(t)$ ..... Second entry of velocity

$\nu_r(t)$ ..... Third entry of velocity

m_{11} ..... (1,1) entry of inertia matrix

m_{22} ..... (2,2) entry of inertia matrix

m_{23} ..... (2,3) entry of inertia matrix

m_{33} ..... (3,3) entry of inertia matrix

d_{11} ..... (1,1) entry of damping matrix

d_{22} ..... (2,2) entry of damping matrix

d_{23} ..... (2,3) entry of damping matrix

d_{32} ..... (3,2) entry of damping matrix

d_{33} ..... (3,3) entry of damping matrix

$z_1(t)$ ..... Position tracking error

$z_2(t)$ . . . . . Auxiliary error

$\alpha(t)$ . . . . . Auxiliary input like term

$Y_d(\eta_d, \dot{\eta}_d, \ddot{\eta}_d)$. Regression matrix in terms of the desired position and its time derivatives

θ . . . . . Uncertain model parameters vector

$\hat{\theta}(t)$ . . . . . Estimate of uncertain model parameters vector

$\tilde{\theta}(t)$ . . . . . Estimation error of θ

$E, D_\ell, F_\ell,\ \ell = 1, ..., h$ Unknown constant diagonal matrix standing for the mean value of the disturbance weights

$\hat{E}(t), \hat{D}_\ell(t), \hat{F}_\ell(t),\ \ell = 1, ..., h$ . . . . . Estimates of E, D_ℓ, F_ℓ

$\tilde{E}(t), \tilde{D}_\ell(t), \tilde{F}_\ell(t),\ \ell = 1, ..., h$ . . . . . Estimation error of E, D_ℓ, F_ℓ

$\varphi, \varphi_\ell,\ \ell = 1, .., h$ . . . . . Constant, diagonal adaptation gain matrices

h . . . . . Harmonic limit of the approximation

Γ . . . . . Positive definite diagonal adaptive gain matrix

$c_{1,2,3}$ . . . . . Positive bounding constants

δ . . . . . Positive damping constant

J . . . . . Dynamic term in robot–like model

C . . . . . Dynamic term in robot–like model

F . . . . . Dynamic term in robot–like model

τ^* . . . . . Control input torque in robot–like model

$Y(\eta, \dot{\eta}, \ddot{\eta})$ . . . . . Regression matrix

Y_d . . . . . Function of desired position

$\gamma(t)$ . . . . . Periodic disturbance term

$e(t)$ . . . . . Position tracking error

$r(t)$ . . . . . Filtered position tracking error

$s(t)$ . . . . . Filtered velocity observation error

μ . . . . . Constant positive gain

t . . . . . Time

$\chi(t)$ . . . . . Auxiliary term

$\tilde{\chi}(t)$ . . . . . Auxiliary error–like term

$\rho_{1,2}\left(\|\cdot\|\right)$ . . . . . Positive bounding function

K_0 . . . . . Constant, positive definite, diagonal control gain matrix

K_1 . . . . . Constant, positive definite, diagonal control gain matrix

K_2 . . . . . Constant, positive definite, diagonal control gain matrix

K_c . . . . . Constant, positive definite, diagonal control gain matrix

K_p . . . . . Constant, positive definite, diagonal control gain matrix

k_n . . . . . Constant, positive scalar damping gain

ρ_{01} . . . . . Known positive bounding constants

ρ_{02} . . . . . Known positive bounding constants

ρ_{03} . . . . . Known positive bounding constants

ρ_{04} . . . . . Known positive bounding constants

ρ_{05} . . . . . Known positive bounding constants

$d_e(t)$ . . . . . Diagonal matrix

$d_{\tanh}(t)$ . . . . . Diagonal matrix

$d_{\cos}(t)$ . . . . . Diagonal matrix

$d_{\sin}(t)$ . . . . . Diagonal matrix

$d_{\text{In}}(t)$ . . . . . Diagonal matrix

$Y_s(e, \dot{e}, \eta_d, \dot{\eta}_d, \ddot{\eta}_d)$ . . . . . Regressor matrix

$\Psi, \Psi_\ell,\ \ell = 1, .., h$ . . . . . Constant, diagonal adaptation gain matrices

$\tilde{\eta}\,(t)$ . . . . . Position observation error

$\dot{\tilde{\eta}}\,(t)$ . . . . . Time derivative of position observation error

$\hat{\eta}\,(t)$ . . . . . Observed position

$\dot{\hat{\eta}}\,(t)$ . . . . . Time derivative of observed position

$p\,(t)$ . . . . . Auxiliary filter vector

$\text{Sgn}(\cdot)$ . . . . . Signum function of matrix

$N_d(\eta, \eta_d, \dot{\eta}_d, \ddot{\eta}_d, t)$ . . . . . Auxiliary term

$N_b(\eta, \dot{\eta}, q_\eta, \dot{\eta}_d, e, r, s, t)$ . . . . . Auxiliary term

$P(t)$ . . . . . Auxiliary non–negative term

λ_1 . . . . . Positive bounding constant

λ_2 . . . . . Positive bounding constant

$z(t)$ . . . . . Combined error vector

$w_0(t)$ . . . . . Auxiliary term

ζ_0 . . . . . Auxiliary term

$q(t)$ . . . . . Auxiliary term

β . . . . . Positive constant

V . . . . . Positive definite, Lyapunov function

$\dot{V}$ . . . . . Time derivative of Lyapunov function

tr$\{\cdot\}$ . . . . . Trace operator

Sat . . . . . Vector form of the standard saturation function

Proj$(\cdot)$ . . . . . Projection operator

$\lambda_{\min}(\cdot)$ . . . . . Minimum eigenvalue

I_n . . . . . Standard identity matrix

LIST OF ABBREVIATIONS

BODY . . . . . Body fixed
DoF . . . . . Degree of freedom
ECEF . . . . . Earth–centered Earth–fixed reference
ECI . . . . . Earth–centered inertial
FSFB . . . . . Full state feedback
GPS . . . . . Global Positioning System
NED . . . . . North–East–Down
OFB . . . . . Output feedback
PD . . . . . Proportional Derivative
PID . . . . . Proportional Integral Derivative

CHAPTER 1

INTRODUCTION

Unmanned surface vessels[1] are used in vast majority of marine applications such as offshore operations, offshore oil and gas drilling, underwater pipeline and cable laying, offshore wind farm constructing turbines, marine rescue and wreck investigation. Therefore the demand for higher accuracy and reliability for ship motion control systems has been increased. The main motivation of developments in this field is mostly to improve marine safety and reduce cost of shipping as well.

Modern marine vessels are equipped with several positioning and/or control systems depending on the applications. These systems may be used for

- position and heading regulation,
- way–point tracking,
- dynamic positioning,
- positioning mooring,
- wave–induced motion reduction,
- managing energy and power systems.

It is commonly agreed on that automatic control of marine vehicles has started with the development of the electrically driven gyroscope that was designed to obtain more reliable navigation systems in these vessels. The early controllers were designed based on the assumption that the system model can be linearized around some operating conditions. After a linear model is obtained, linear control techniques were then applied. Among those controllers there are linear optimal controllers as in Balchen et al. (1976), Grimble et al. (1980), Sørensen et al. (1996), Fossen and Grovlen (1998), proportional integral derivative (PID) type controllers as in Balchen et al. (1980).

[1] Throughout this thesis, the terms marine vessel/vehicle, surface vessel/vehicle, ship, craft will be used interchangeably.

PID control is the most popular method to control a system. In fact, PID controller was discovered to automate ship steering in the first place (Ang et al., 2005). Even though the PID controller was used, there was a common problem of almost all actuators which is the inability to realize high frequency input signals. Therefore the input signals are required to be filtered before being applied to the actuators. For filtering purposes, in early course–keeping autopilots, low–pass and notch filters were used. Unfortunately, due to filtering out high frequency signals, they introduced noticeable phase lag and this resulted in performance degradation (Fossen and Perez, 2009). An alternative solution to this problem came with the design of Kalman filter which was used as an observer to separate the wave motion from the low frequency motion in Fossen and Perez (2009). In Balchen et al. (1980), a Kalman filter was used in a linearised system for optimal estimation of vessel motions and environmental forces. Even though disturbances varied with weather conditions and Kalman filter gain needed to be adjusted for each alteration, the proposed Kalman filter was capable of adapting to these varying conditions. Fung and Grimble (1983) proposed a modification to the Kalman filter by adding a self–tuning feature to adjust the filter matrices which yielded better results.

Furthermore, robustness is still another crucial problem of the marine vessel controllers. H_∞ is a linear control method that can improve robustness that can be obtained with Kalman filtering or similar methods. In Katebi et al. (2001), H_∞ controller was designed to compensate for the disturbances of an approximate linear model derived by linearizing the nonlinear hydrodynamic equations.

PID controller is one of the traditional ways to control the system (Balchen et al., 1980). Even though the structure of PID controllers is simple and they are easy to implement, having manually adjusted constant gains may limit the regulation performance. Additionally, these controllers cannot usually compensate for the negative effects of varying external forces since the controller gains are commonly constant and cannot change with the change of disturbances. One approach to address this problem was employing intelligent techniques such as neural networks and genetic algorithms. In Yunsheng et al. (2015), fuzzy logic based self–tuning PID controller was proposed. This online tuning of PID gains provided more flexibility, adaptability and improved robustness.

Although a certain amount of success was achieved with these approaches, it was clear that compensation of nonlinear dynamic model was not always possible via the use

of linear controllers on neither linearized nor nonlinear model. Moreover when system uncertainties and external disturbances are taken into consideration, it becomes apparent that the controller for the unmanned marine vehicles should be able to cope with external disturbances and compensate for the nonlinearities in the system dynamics. Therefore the problems caused by linearization motivated researchers to apply nonlinear control techniques to the nonlinear system model.

Some past research on control of marine vessels has focused on designing exact model knowledge controllers that relied on accurate knowledge of the system model (Fossen, 2002). However modeling uncertainties should be appropriately addressed as they are common in almost all systems. Adaptive control techniques are the preferred method to compensate for parametric uncertainties in the system model (Fossen, 2002). However marine vessels are usually subject to other anomalies such as environmental effects which mandate the use of robust control approaches either alone or in conjunction with adaptive techniques.

Some line of past research has focused on designing robust controllers for different research problems. In Bidikli et al. (2017a), robust control of dynamically positioned surface vessel was proposed to compensate system uncertainties while ensuring asymptotic tracking. Robust adaptive finite time tracking controller was used for trajectory tracking control of a fully actuated marine vessel in Wang et al. (2015). In Zhang et al. (2017), a path–following controller obtained by fusing Kalman filter, disturbance observer, and robust control method was presented for underactuated surface vessels to compensate for uncertain system model and disturbances. In Zhu and Du (2018), trajectory tracking control problem of surface ships in the presence of parametric uncertainties, time–varying disturbances and input saturation was solved via a robust adaptive control approach. Robust adaptive control approach was the preferred method in Hu et al. (2017) and Liao et al. (2020) where similar research problems were addressed. Utilization of a nonlinear proportional–derivative (PD) type controller for dynamic positioning of vehicles in 6 degrees of freedom was researched in Fjellstad and Fossen (1994). Besides, utilization of sliding mode controllers for the control of unmanned surface vessels were also examined in Tannuri and Agostinho (2010), Qiao and Zhang (2018), Chen et al. (2020). In Tannuri et al. (2001) and Agostinho et al. (2009), nonlinear sliding mode technique was also used for position control of vessels . Although sliding mode control is capable of compensating

for model uncertainties theoretically, but as in all sliding mode controllers, it suffers from the chattering problem. This undesirable effect avoids sliding mode type controllers to be used in real systems and can only be reduced with high order sliding mode controller (Tannuri and Agostinho, 2010).

In the control literature review above, only full state feedback controllers were mentioned. For reliable measurements of position and velocity, information can be collected from sensors, such as GPS, differential GPS, speed log, compass, gyros, radar, and accelerometers (Fossen and Perez, 2009). However, many surface vessels do not possess this equipment to obtain reliable velocity measurements, besides the devices may not work properly under some conditions. Thus the absence of velocity measurement becomes a restriction that must be appropriately addressed.

Observer–based control designs were considered as feasible solutions to cope with the lack of measurements of some states. Motivated by this, Fossen and Grovlen (1998) presented a nonlinear model based output feedback controller using an observer backstepping method in order to eliminate the need for velocity measurements. Loria et al. (2000) proposed a globally asymptotically stabilizing controller when the position measurements are noisy. In Wondergem et al. (2010), an observer based controller for fully actuated ships was proposed when the exact knowledge of the system parameters are available. A nonlinear model–free observer based control approach was utilized in Bidikli et al. (2013). In addition to the aforementioned works, in Bidikli et al. (2017b), Wang et al. (2019), Lu et al. (2020) observer based adaptive controllers were designed. In addition to the observer–based techniques, a series of filters can be preferred to tackle the problem caused by the unmeasurable states without observing them. This method is called filter–based output feedback control. Fang et al. (2004) designed a velocity surrogate filter–based output feedback adaptive controller that did not need exact knowledge of the ship dynamics. The above mentioned works either required exact model knowledge of system dynamics for control or observer design or for both, or compensated only for parametric uncertainties.

As emphasized in the literature, when designing controllers for marine vehicles, both parametric uncertainties and environmental forces must be considered. Nonlinear robust control techniques are usually preferred when dealing with modeling anomalies. But robust controllers that are designed to compensate for uncertain system dynamics

by ignoring the dynamics can yield to degraded performance. Furthermore, usually a function depending on a conservatively determined upper bound of the uncertain system dynamics is used as part of the robust control input design and this requires excessively higher control efforts. Utilizing adaptive components to deal with parametric uncertainties in conjunction with robust controllers can help but cannot fully overcome both of the above mentioned issues.

The main aim of this thesis is to design trajectory tracking controllers for marine vessels. Since parameters in the dynamic model of the ship are not always known, this issue should be considered in design of controllers. In addition to that, environmental forces have a negative impact on the motion of surface vessels and thus should be appropriately dealt with. In accordance with a recent line of research on control of marine vehicles, the environmental disturbances are considered to be periodic as a direct consequence of the natural response of the oceanic waves. Specifically, in Du et al. (2018), when designing controllers for marine vehicles, it was considered that the dynamic model was subject to unknown time–varying disturbances that can be expressed as the superposition of a series of sinusoidal components. The research topic of this thesis was actually decided after this publication was studied. However, the design in Du et al. (2018) was complicated and an alternative periodic disturbance estimation tool that could be utilized as part of the control input torque was required to be designed. When a system is subject to periodic disturbances, in the literature, the mainly preferred method is repetitive learning controllers. Despite their high performance when dealing with periodic uncertainties, repetitive learning controllers require the exact knowledge of the period of the uncertain periodic terms. While for some systems the period may be available or can be easily obtained, it is not the case for the oceanic waves. Thus repetitive learning controllers could not be utilized to address the problem at hand.

In (Du et al., 2018), it was stated that low frequency disturbances can be separated as sinusoidal terms with different frequencies, amplitudes and phases as a result of the Fourier representation, and having inspired mainly from Du et al. (2018), an alternative approach, by using a Fourier series expansion–like method was utilized to model the additive periodic environmental forces. Specifically, in this thesis, a novel approach for unmanned surface vessels has been utilized to deal with external disturbances which exploits the periodicity property of the oceanic waves using Fourier series expansion–like

method. Additionally, the presence of parametric uncertainties in the dynamic model of the ships must also be addressed. Under these restrictions, tracking control of surface vessels is considered in two different scenarios depending on the availability of velocity measurements. In the first part, backstepping control technique is utilized to design a robust control structure supported with the Fourier series expansion–like periodic disturbance estimation method when full–state feedback is available (*i.e.*, when both position and velocity measurements are available for control design). In the second part, by utilizing the fact that the nonlinear ship model can be arranged similar to a robot manipulator dynamic model, a desired ship model based controller formulation in conjunction with a model–independent velocity observer (*i.e.*, the observer formulation does not require system parameters) is designed to cope with the lack of velocity measurement since the position of the ship is the only measurable state. For compensating the periodic disturbance effects, the proposed method was used with a modification since velocity feedback is not available. For both controllers, the stability of the closed–loop system and the convergence of the tracking errors are investigated via Lyapunov based tools. The theoretical findings are backed up by extensive numerical simulations where performance evaluations are also shown for different scenarios.

The organization of the remaining part of this thesis is arranged in the following manner. Chapter 2 represents kinematics and dynamics of ship motion. In Chapter 3, full state feedback backstepping controller is proposed for position tracking of unmanned surface vessels while the periodic environmental forces are compensated with the periodic disturbance estimation method inspired from Fourier series expansion. In Chapter 4, observer based adaptive robust control supported with periodic disturbance estimation method is studied for position tracking of unmanned surface vessels when position is the only available state and periodic disturbances affect the system. Control input design, stability analysis and simulation results are conducted for each study. It is emphasized the presentations of Chapter 3 and 4, which contain the main research outputs, are arranged to be self–contained. In Chapter 5, the results obtained during the course of research efforts are summarized and some possible future works are also discussed.

CHAPTER 2

MODELING OF MARINE VESSELS

To understand the behaviour of the motion of the ship, the mathematical model is investigated in two parts which are kinematics and dynamics. Kinematics associate with the geometrical aspects of the motion, or in other words, translation of motion between different frames of references whereas dynamics analyse the forces causing the motion (Fossen, 2002).

The full order ship motion is defined by 6 degree of freedom which corresponds to 6 independent coordinates being required to determine positions and orientations. The first three coordinates and their time derivatives represent the position and translational motion along the x, y, and z axes while the other 3 coordinates and their time derivatives correspond to the orientation and rotational motions. These components are defined as *surge*, *sway*, *heave*, *roll*, *pitch*, and *yaw* (Fossen, 2002).

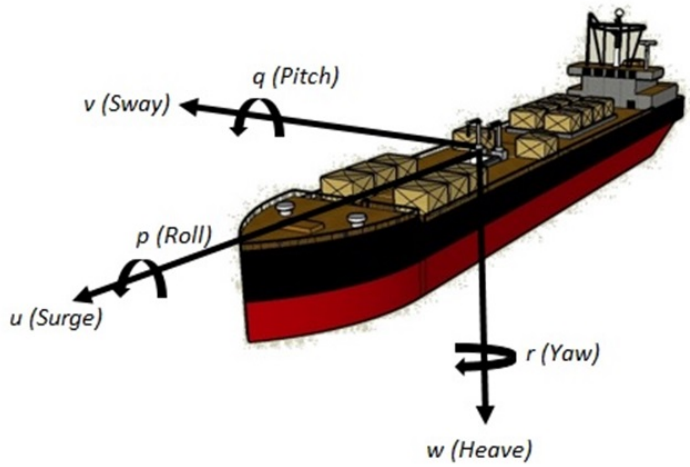

Figure 2.1. Motion variables for a marine vessel.

The mathematical model for the dynamically positioned ship describing the low–frequency motion has the following general form

$$\dot{\eta} = R\nu \tag{2.1}$$

$$M\dot{\nu} + C_c\nu + D\nu + \tau_d = \tau. \tag{2.2}$$

The model in (2.1) is referred to as the kinematic model while (2.2) represents the dynamic model. In the above model, $\eta(t)$ and $\nu(t)$ denote the position and the velocity of the ship, respectively. In (2.1), $R(\eta)$ represents the orthogonal rotation matrix between the Earth and body–fixed coordinate frames. In (2.2), M is the inertia matrix that determines the force needed for a desired acceleration. The Coriolis and centripetal terms shown with C_c, are used to express the motion within the body–fixed reference frame with respect to the inertial frame. This term is taken into account when the vessel performs rotational motion maneuvers, otherwise its contribution is usually neglected. Furthermore, for ships having low cruise speeds Coriolis force can be ignored (Wondergem et al., 2010). Matrix D models the hydrodynamic damping forces describing the moments acting on the vessel. In (2.2), $\tau(t)$ is the control input torque and $\tau_d(t)$ represents low–frequency environmental forces due to wind, waves and ocean currents. As discussed in Chapter 1, even though high–frequency wave induced forces also impact the vessel, these terms are not usually considered in the control loop since vessel actuators are not able to cancel their effects. As detailed previously in Chapter 1, various filtering techniques have been offered to avoid unnecessary wear and tear (Fossen and Strand, 1999a), (Fung and Grimble, 1983), (Hassani et al., 2012). On the other hand it is not always crucial to compensate the effects of wave frequency disturbances since they give rise to the ship's back–and–forth rocking motions (Veksler et al., 2016).

Examining the past research on vessel modeling reveals that models with different degree of freedom are utilized in control systems. According to the motions of the craft, they can be categorized as follows:

- **1 DoF** models are used to design forward (*surge*), heading (*yaw*), or roll (*roll*) motion controllers (Li and Sun, 2011).

- **3 DoF** models which are the most commonly preferred ones are used for different control objectives such that dynamic positioning, tracking control and path–following systems in horizontal plane (*surge*, *sway* and *yaw*), longitudinal (*surge*, *heave* and *pitch*), or lateral (*sway*, *roll* and *yaw*) models. Stabilization of the *surge*, *sway* and *yaw* modes are required for marine vessels to maintain desired positions.

- **4 DoF** models (*surge*, *sway*, *yaw* and *roll*) are used in maneuvering situations and usually formed by adding the roll equation to the 3 DoF horizontal plane model (Perez and Blanke, 2010).

- **6 DoF** models (*surge*, *sway*, *heave*, *roll*, *pitch* and *yaw*) are used for modeling of fully coupled vehicle motions. These models are preferred for controlling fully actuated vehicles (Fossen, 2011).

In this study, the vertical dynamics will be ignored and the most common model that is the horizontal 3 degree of freedom model will be used in the subsequent chapters. The main reason of preferring reduced–order models in designing controllers for marine vehicles is that most vessels do not have actuation in all degrees of freedom.

As already mentioned at the beginning of this section, kinematics is the science describing the geometrical relationships of the motion. The ship's motions are described by two reference frames, a local geographical Earth–fixed frame and a body–fixed frame. The common reference frames used for depicting the motion of the ship are summarized below.

- **Earth–Centered Reference Frames**

  - The Earth–centered inertial (ECI) frame has its origin at the center of the earth and do not remain fixed with respect to Earth's surface in its rotation. Hence, this reference frame is preferred for representing the motion of objects in space.

  - The Earth–centered Earth–fixed reference (ECEF) frame has its origin at the center of the earth similar to the ECI; however, in contrast to ECI, it rotates with respect to the stars. Thus, it is suitable for describing the position or velocity of a terrestrial object.

- **Geographical Reference Frames**

  - North–East–Down (NED) is a reference frame which is fixed to a point on the earth surface. For this system, the x–axis points towards true north whereas the y–axis points towards east, therefore z–axis points downwards. This is the coordinate frame we use commonly in our daily life.

– Body fixed (BODY) frame is attached to the vessel under consideration and moves with the craft. Since it moves with the vessel, it is usually not used for representing the vessel position and orientation. Generally the position and orientation of the vessel are expressed in the NED or ECEF reference frame while the body–fixed coordinate system is referred to describe the linear and angular velocities of the vessel (Fossen, 2002).

Relation between the earth–fixed NED frame and the vessel–fixed BODY frame is illustrated in Figure 2.2 while Figure 2.3 shows the ECI, ECEF, and NED reference frames in the same figure.

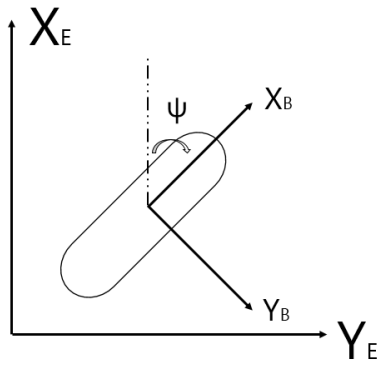

Figure 2.2. Relation between the NED frame and the BODY frame.

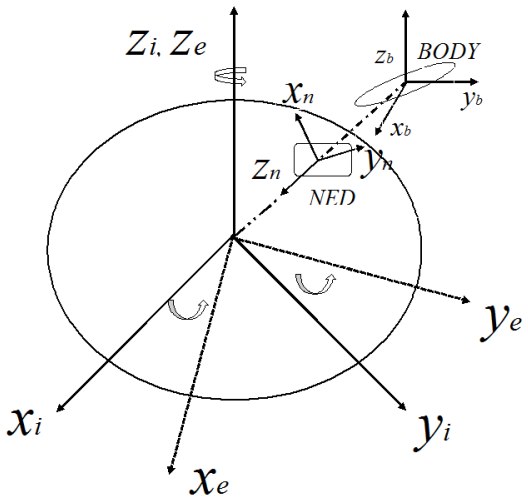

Figure 2.3. Illustration of the ECI, ECEF, and NED reference frames.

CHAPTER 3

FULL STATE FEEDBACK APPROACH

In this chapter, tracking control of surface vessels in the presence of parametric uncertainties and additive periodic disturbances is considered. For estimation of environmental forces, periodic disturbance estimation method inspired from Fourier series expansion have been applied. Stability of the closed–loop system and the convergence of the tracking error under the closed–loop operation are established via Lyapunov based arguments. Simulation studies are provided to support the theoretical results and demonstrate the effectiveness of the proposed method.

This chapter is organized as follows: Dynamic model of a 3 degree of freedom surface vessel is represented in Section 3.1 while Section 3.2 shows the error system development and the control design. In Section 3.3, stability analysis of the proposed control strategy is presented. Numerical simulation results are presented in Section 3.4 and Section 3.5 contains concluding remarks.

3.1. System Model and Properties

The mathematical model for the dynamically positioned ship has the following form (Fossen, 2002)

$$\dot{\eta} = R\nu \tag{3.1}$$

$$M\dot{\nu} + D\nu + \tau_d = \tau \tag{3.2}$$

where $\eta(t)$, $\nu(t) \in \mathbb{R}^3$ denote the position and the velocity of the ship, respectively, $M \in \mathbb{R}^{3\times3}$ is the inertia matrix, $D \in \mathbb{R}^{3\times3}$ is the damping matrix, $\tau_d(t) \in \mathbb{R}^3$ denotes the uncertain additive periodic disturbance, $\tau(t) \in \mathbb{R}^3$ is the vector of control inputs and $R(\eta) \in \mathbb{R}^{3\times3}$ represents the orthogonal rotation matrix between the Earth and body–fixed coordinate frames. The position and velocity vectors are in the form $\eta \triangleq [\ x(t) \quad y(t) \quad \psi(t)\ ]^T$ and $\nu = [\ \nu_u(t) \quad \nu_v(t) \quad \nu_r(t)\ ]^T$, respectively, where $x(t)$,

$y(t) \in \mathbb{R}$ denote the translational positions, $\psi(t) \in \mathbb{R}$ is the rotation about yaw axes of the ship, while $\nu_u(t)$, $\nu_v(t) \in \mathbb{R}$ represent the translational velocities and $\nu_r(t) \in \mathbb{R}$ is the rotational velocity about the yaw axes.

After taking the time derivative of (3.1) and using the orthogonality property of the rotation matrix, the following expression is obtained

$$\dot{\nu} = R^T(\ddot{\eta} - \dot{R}R^T\dot{\eta}). \tag{3.3}$$

Therefore, (3.2) can be rewritten as

$$MR^T(\ddot{\eta} - \dot{R}R^T\dot{\eta}) + DR^T\dot{\eta} + \tau_d = \tau. \tag{3.4}$$

In view of (3.4), the mathematical model of the ship consisting of the desired position $\eta_d(t) \in \mathbb{R}^3$ and its time derivates can be written as follows

$$Y_d\theta = MR^T(\eta_d)[\ddot{\eta}_d - \dot{R}(\eta_d)R^T(\eta_d)\dot{\eta}_d] + DR^T(\eta_d)\dot{\eta}_d \tag{3.5}$$

where $Y_d(\eta_d, \dot{\eta}_d, \ddot{\eta}_d) \in \mathbb{R}^{3\times 9}$ is a function of the desired position and its time derivatives and $\theta \in \mathbb{R}^9$ is an uncertain parameter vector.

3.2. Error System Development and Control Input Design

Our control objective is to make $\eta(t)$ track a sufficiently smooth, bounded desired trajectory under the restrictions that the dynamic model is uncertain and is subject to additive uncertain periodic disturbances.

The position tracking error, denoted by $z_1(t) \in \mathbb{R}^3$, is defined as

$$z_1 \triangleq \eta - \eta_d. \tag{3.6}$$

An auxiliary error, denoted by $z_2(t) \in \mathbb{R}^3$, is defined as

$$z_2 \triangleq \nu - \alpha \tag{3.7}$$

where $\alpha(t) \in \mathbb{R}^3$ is an auxiliary input like term designed as

$$\alpha = R^T(\dot{\eta}_d - K_1 z_1) \tag{3.8}$$

where $K_1 \in \mathbb{R}^{3\times3}$ is a positive definite diagonal control gain matrix. Substituting (3.7) and (3.8) into the time derivative of (3.6) yields

$$\dot{z}_1 = -K_1 z_1 + R z_2 \tag{3.9}$$

where (3.1) and orthogonality of $R(\eta)$ were made use of. Following the footsteps of the literature on backstepping based control design (Kokotovic, 1992), (Fossen and Strand, 1999b) for the stability analysis, a non–negative function, denoted by $V_1(t) \in \mathbb{R}^3$, is considered

$$V_1 \triangleq \frac{1}{2} z_1^T z_1. \tag{3.10}$$

The time derivative of $V_1(t)$ is obtained as

$$\dot{V}_1 = -z_1^T K_1 z_1 + z_1^T R z_2 \tag{3.11}$$

where (3.9) was substituted.

To obtain the dynamics for $z_2(t)$, taking the time derivative of $z_2(t)$ yields

$$\dot{z}_2 = \dot{\nu} - \dot{\alpha}. \tag{3.12}$$

The time derivative of (3.8) is taken to obtain

$$\dot{\alpha} = \dot{R}^T(\dot{\eta}_d - K_1 z_1) + R^T(\ddot{\eta}_d - K_1 \dot{z}_1) \tag{3.13}$$

which contains the time derivative of rotation matrix obtained as $\dot{R} = RS(\nu_r)$ where $S(\nu_r) \in \mathbb{R}^{3\times3}$ is a skew–symmetric matrix defined as

$$S(\nu_r) \triangleq \begin{bmatrix} 0 & -\nu_r & 0 \\ \nu_r & 0 & 0 \\ 0 & 0 & 0 \end{bmatrix}. \tag{3.14}$$

By utilizing $S^T = -S$, the time derivative of α is rearranged as

$$\dot{\alpha} = -SR^T\dot{\eta}_d + SR^TK_1z_1 + R^T\ddot{\eta}_d - R^TK_1\dot{\eta} + R^TK_1\dot{\eta}_d. \tag{3.15}$$

Premultiplying (3.12) with M and utilizing (3.2) and (3.15) yields

$$\begin{aligned} M\dot{z}_2 &= \tau - D\nu - \tau_d + MSR^T\dot{\eta}_d - MSR^TK_1z_1 \\ &\quad -MR^T\ddot{\eta}_d + MR^TK_1\dot{\eta} - MR^TK_1\dot{\eta}_d. \end{aligned} \tag{3.16}$$

To obtain a compact form of (3.16), $W(\eta, \nu, \eta_d, \dot{\eta}_d, \ddot{\eta}_d) \in \mathbb{R}^{3\times p}$ is introduced as

$$\begin{aligned} W\theta &= D\nu - MSR^T\dot{\eta}_d + MSR^TK_1z_1 + MR^T\ddot{\eta}_d \\ &\quad -MR^TK_1\dot{\eta} + MR^TK_1\dot{\eta}_d \end{aligned} \tag{3.17}$$

with which (3.16) is rewritten as

$$M\dot{z}_2 = \tau - \tau_d - W\theta. \tag{3.18}$$

In (3.17), θ is the same uncertain parameter vector introduced in (3.5).

Assumption 1 *In view of the Fourier series expansion–like technique (Delibasi et al., 2006), (Delibasi et al., 2010), the periodic disturbances are assumed to be written as*

$$\tau_d = E^T\mathit{Tanh}(z_2) + \sum_{\ell=1}^{h} D_\ell^T\mathit{Cos}(\ell z_2) + \sum_{\ell=1}^{h} F_\ell^T\mathit{Sin}(\ell z_2) \tag{3.19}$$

where $E \in \mathbb{R}^{3\times3}$ is unknown, mean value disturbance weight matrix, $D_\ell, F_\ell \in \mathbb{R}^{3\times3}$, $\ell = 1, .., h$ are constant matrices with unknown parameters and $h \in \mathbb{R}^+$ is harmonic limit

of the approximation with $\ell = 1, .., h$ representing different error frequencies where the vector forms of sinusoidal functions are obtained as

$$\begin{aligned} \textit{Tanh}(z_2) &= [\ \tanh(z_{21}) \quad \tanh(z_{22}) \quad \tanh(z_{23})\ ]^T && (3.20) \\ \textit{Sin}(\ell z_2) &= [\ \sin(\ell z_{21}) \quad \sin(\ell z_{22}) \quad \sin(\ell z_{23})\ ]^T && (3.21) \\ \textit{Cos}(\ell z_2) &= [\ \cos(\ell z_{21}) \quad \cos(\ell z_{22}) \quad \cos(\ell z_{23})\ ]^T && (3.22) \end{aligned}$$

for $z_2(t) = [\ z_{21} \quad z_{22} \quad z_{23}\ ]^T$.

Substituting (3.19) into (3.18) yields

$$M\dot{z}_2 = -W\theta + \tau - E^T \text{Tanh}(z_2) - \sum_{\ell=1}^{h} D_\ell^T \text{Cos}(\ell z_2) - \sum_{\ell=1}^{h} F_\ell^T \text{Sin}(\ell z_2). \quad (3.23)$$

Based on the subsequent stability analysis, the control input is designed as

$$\tau = -K_2 z_2 - R^T z_1 + Y_d \hat{\theta} + \hat{E}^T \text{Tanh}(z_2) + \sum_{\ell=1}^{h} \hat{D}_\ell{}^T \text{Cos}(\ell z_2) + \sum_{\ell=1}^{h} \hat{F}_\ell{}^T \text{Sin}(\ell z_2) \quad (3.24)$$

where $K_2 \in \mathbb{R}^{3\times3}$ is a positive definite control gain matrix, $\hat{\theta}(t) \in \mathbb{R}^9$ is the estimate of uncertain model parameters, $\hat{E}(t) \in \mathbb{R}^{3\times3}$, $\hat{D}_\ell(t) \in \mathbb{R}^{3\times3}$, $\hat{F}_\ell(t) \in \mathbb{R}^{3\times3}$ stand for the estimates of E, D_ℓ and F_ℓ for $\ell = 1, .., h$, respectively, and are designed as follows

$$\begin{aligned} \dot{\hat{\theta}} &= -\Gamma Y_d^T z_2 && (3.25) \\ \dot{\hat{E}} &= -\varphi \text{Tanh}(z_2) z_2^T && (3.26) \\ \dot{\hat{D}}_\ell &= -\varphi_\ell \text{Cos}(\ell z_2) z_2^T, \ell = 1, .., h && (3.27) \\ \dot{\hat{F}}_\ell &= -\varphi_\ell \text{Sin}(\ell z_2) z_2^T, \ell = 1, .., h && (3.28) \end{aligned}$$

where $\Gamma \in \mathbb{R}^{9\times9}$, φ, $\varphi_\ell \in \mathbb{R}^{3\times3}$ $\ell = 1, ..h$ are positive definite, diagonal adaptive gain matrices. The flow diagram of the closed–loop system under the control input in (3.24) is presented in Figure 3.1.

The terms in the control input design in (3.24) are now briefly discussed. The term $-K_2 z_2$ is a feedback term while $-R^T z_1$ is introduced to cancel a cross term in Lyapunov analysis that comes from the z_1 dynamics as in (3.11). The adaptive term $Y_d \hat{\theta}$ is designed to

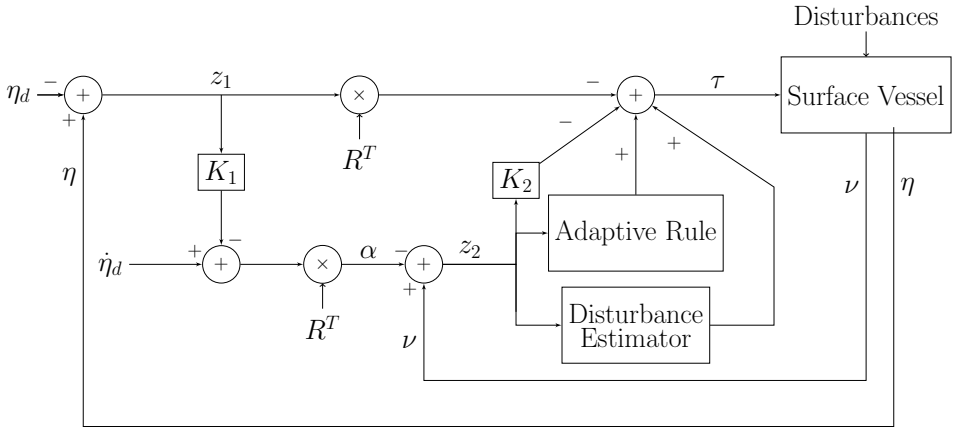

Figure 3.1. Flow diagram of the FSFB controller in (3.24).

compensate for the uncertain model parameters in an adaptive manner while the remaining terms are for estimating the uncertain additive periodic disturbances.

After substituting (3.24) into (3.23), the closed–loop error system for z_2 yields

$$\begin{aligned} M\dot{z}_2 = & - W\theta + Y_d\hat{\theta} - K_2 z_2 - R^T z_1 - \tilde{E}^T \text{Tanh}(z_2) \\ & - \sum_{\ell=1}^{h} \tilde{D}_\ell^T \text{Cos}(\ell z_2) - \sum_{\ell=1}^{h} \tilde{F}_\ell^T \text{Sin}(\ell z_2) \end{aligned} \tag{3.29}$$

where $\tilde{\theta}(t) \in \mathbb{R}^9$, $\tilde{E}(t)$, $\tilde{D}_\ell(t)$, $\tilde{F}_\ell(t) \in \mathbb{R}^{3\times 3}$ $\ell = 1, .., h$ are defined as

$$\tilde{\theta} \triangleq \theta - \hat{\theta} \tag{3.30}$$

$$\tilde{E} \triangleq E - \hat{E} \tag{3.31}$$

$$\tilde{D}_\ell \triangleq D_\ell - \hat{D}_\ell \tag{3.32}$$

$$\tilde{F}_\ell \triangleq F_\ell - \hat{F}_\ell. \tag{3.33}$$

To quantify the difference between the previously defined parametrizations $Y_d\theta$ and $W\theta$, the auxiliary term $\chi(\cdot) \in \mathbb{R}^3$ is defined as

$$\chi \triangleq Y_d\theta - W\theta \tag{3.34}$$

whose norm can be proven to be upper bounded as

$$\|\chi\| \leq c_1\|z_1\| + c_2\|z_2\| + c_3\|z_1\|^2 + c_4\|z_1\|\|z_2\| \tag{3.35}$$

where $c_1, c_2, c_3, c_4 \in \mathbb{R}$ are positive bounding constants. In Appendix A, the bound of $\left\|\chi(t)\right\|$ in (3.35) is presented. In view of (3.34), (3.29) is obtained as

$$\begin{aligned} M\dot{z}_2 &= \chi - Y_d\tilde{\theta} - K_2 z_2 - R^T z_1 - \tilde{E}^T \text{Tanh}(z_2) \\ &\quad - \sum_{\ell=1}^{h} \tilde{D}_\ell^T \text{Cos}(\ell z_2) - \sum_{\ell=1}^{h} \tilde{F}_\ell^T \text{Sin}(\ell z_2) \end{aligned} \tag{3.36}$$

where $Y_d\theta$ was added and subtracted.

3.3. Stability Analysis

Theorem 3.3.1 *The control input in* (3.24) *in conjunction with the adaptive update rule in* (3.25) *and the estimation of the periodic disturbance parameters in* (3.26)–(3.28) *ensures asymptotic stability of the closed–loop system in the sense that*

$$\left\|z_1(t)\right\|, \left\|z_2(t)\right\| \to 0 \text{ as } t \to \infty \tag{3.37}$$

provided that

$$\min(\lambda_{\min}(K_1), \lambda_{\min}(K_2)) > \max\left(\frac{c_1}{2} + \frac{c_3 V(0)}{2\delta} + c_4\delta, \frac{c_1}{2} + c_2 + c_3\delta + \frac{c_4 V(0)}{2\delta\lambda_{\min}(M)}\right) \tag{3.38}$$

is satisfied where δ is a positive damping constant and $V(0)$ represents the initial value of the subsequently designed Lyapunov function $V(t)$.

Proof To prove the above result, the non–negative Lyapunov function, denoted with $V(z_1, z_2, \tilde{\theta}, \tilde{E}, \tilde{D}_k, \tilde{F}_\ell) \in \mathbb{R}$, is defined as

$$\begin{aligned} V &\triangleq V_1 + \frac{1}{2} z_2^T M z_2 + \frac{1}{2}\tilde{\theta}^T \Gamma^{-1} \tilde{\theta} + \frac{1}{2}\text{tr}\{\tilde{E}^T \varphi^{-1} \tilde{E}\} \\ &\quad + \frac{1}{2}\text{tr}\left\{\sum_{\ell=1}^{h} \tilde{D}_\ell^T \varphi_\ell^{-1} \tilde{D}_\ell\right\} + \frac{1}{2}\text{tr}\left\{\sum_{\ell=1}^{h} \tilde{F}_\ell^T \varphi_\ell^{-1} \tilde{F}_\ell\right\} \end{aligned} \tag{3.39}$$

where $\text{tr}\{\cdot\}$ is the trace operator. The time derivative of the Lyapunov function (3.39) is obtained as

$$\begin{aligned}\dot{V} &= \dot{V}_1 + z_2^T M \dot{z}_2 + \tilde{\theta}^T \Gamma^{-1} \dot{\tilde{\theta}} + \text{tr}\{\tilde{E}^T \varphi^{-1} \dot{\tilde{E}}\} \\ &\quad + \text{tr}\left\{ \sum_{\ell=1}^{h} \tilde{D}_\ell^T \varphi_\ell^{-1} \dot{\tilde{D}}_\ell \right\} + \text{tr}\left\{ \sum_{\ell=1}^{h} \tilde{F}_\ell^T \varphi_\ell^{-1} \dot{\tilde{F}}_\ell \right\}. \end{aligned} \tag{3.40}$$

Utilizing (3.11), (3.36) and the time derivatives of (3.30)–(3.33) along with θ, E, D_ℓ, F_ℓ being constant and the update rules in (3.25)–(3.28) yields

$$\begin{aligned}\dot{V} &= -z_1^T K_1 z_1 + z_1^T R z_2 + z_2^T \Big[\chi - Y_d \tilde{\theta} - K_2 z_2 - R^T z_1 - \tilde{E}^T \text{Tanh}(z_2) \\ &\quad - \sum_{\ell=1}^{h} \tilde{D}_\ell^T \text{Cos}(\ell z_2) - \sum_{\ell=1}^{h} \tilde{F}_\ell^T \text{Sin}(\ell z_2) \Big] + \tilde{\theta}^T Y_d^T z_2 + \text{tr}\{\tilde{E}^T \text{Tanh}(z_2) z_2^T\} \\ &\quad + \text{tr}\left\{ \sum_{\ell=1}^{h} \tilde{D}_\ell^T \text{Cos}(\ell z_2) z_2^T \right\} + \text{tr}\left\{ \sum_{\ell=1}^{h} \tilde{F}_\ell^T \text{Sin}(\ell z_2) z_2^T \right\}. \end{aligned} \tag{3.41}$$

Canceling common terms and by using the trace property $\text{tr}\{a^T b c^T\} = \text{tr}\{c^T a^T b\}$, $\dot{V}$ is rearranged as

$$\dot{V} = -z_1^T K_1 z_1 + z_2^T \chi - z_2^T K_2 z_2. \tag{3.42}$$

By utilizing (3.35), the upper bound for the right hand side of (3.42) can be obtained as

$$\begin{aligned}\dot{V} &\leq -\lambda_{\min}\{K_1\}\|z_1\|^2 - \lambda_{\min}\{K_2\}\|z_2\|^2 + c_1\|z_1\|\|z_2\| + c_2\|z_2\|^2 \\ &\quad + c_3\|z_1\|^2\|z_2\| + c_4\|z_1\|\|z_2\|^2 \end{aligned} \tag{3.43}$$

and utilizing Young's inequality yields

$$\begin{aligned}\dot{V} &\leq -\lambda_{\min}\{(K_1)\}\|z_1\|^2 - \lambda_{\min}\{(K_2)\}\|z_2\|^2 + \frac{c_1}{2}\|z_1\|^2 + \frac{c_1}{2}\|z_2\|^2 \\ &\quad + c_2\|z_2\|^2 + \frac{c_3}{4\delta}\|z_1\|^4 + c_3\delta\|z_2\|^2 + \frac{c_4}{4\delta}\|z_2\|^4 + c_4\delta\|z_1\|^2. \end{aligned} \tag{3.44}$$

Combining the common terms results in

$$\begin{aligned}\dot{V} &\leq -\left[\lambda_{\min}(K_1) - \frac{c_1}{2} - \frac{c_3}{4\delta}\|z_1\|^2 - c_4\delta\right]\|z_1\|^2 \\ &\quad - \left[\lambda_{\min}(K_2) - \frac{c_1}{2} - c_2 - c_3\delta - \frac{c_4}{4\delta}\|z_2\|^2\right]\|z_2\|^2. \end{aligned} \tag{3.45}$$

In view of (3.11) and (3.39), a more conservative bound can be obtained as

$$\begin{aligned}\dot{V} \;\leq\; & -\Big[\lambda_{\min}(K_1) - \frac{c_1}{2} - \frac{c_3}{4\delta}2V(t) - c_4\delta\Big]\|z_1\|^2 \\ & -\Big[\lambda_{\min}(K_2) - \frac{c_1}{2} - c_2 - c_3\delta - \frac{c_4}{4\delta}\frac{2V(t)}{\lambda_{\min}(M)}\Big]\|z_2\|^2 \end{aligned} \tag{3.46}$$

and provided that

$$\min(\lambda_{\min}(K_1), \lambda_{\min}(K_2)) - \max\Big(\frac{c_1}{2} + \frac{c_3 V}{2\delta} + c_4\delta, \frac{c_1}{2} + c_2 + c_3\delta + \frac{c_4 V}{2\delta\lambda_{\min}(M)}\Big) > 0 \tag{3.47}$$

is satisfied then

$$\dot{V} \leq -\beta(\|z_1\|^2 + \|z_2\|^2) \tag{3.48}$$

for some $\beta > 0$. Since the maximum value $V(t)$ can take is its initial value $V(0)$, from (3.47), a more conservative gain condition is obtained as

$$\min(\lambda_{\min}(K_1), \lambda_{\min}(K_2)) > \max\Big(\frac{c_1}{2} + \frac{c_3 V(0)}{2\delta} + c_4\delta, \frac{c_1}{2} + c_2 + c_3\delta + \frac{c_4 V(0)}{2\delta\lambda_{\min}(M)}\Big). \tag{3.49}$$

From the structures of (3.39) and (3.48), provided (3.49) is satisfied then $V(t) \in \mathcal{L}_\infty$ and thus $z_1(t), z_2(t), \tilde{\theta}(t), \tilde{E}(t), \tilde{D}_\ell(t), \tilde{F}_\ell(t), \ell = 1, .., h$ are bounded. These boundedness statements can be used with the boundedness of the desired trajectory and its time derivatives to prove that $\eta(t), \alpha(t) \in \mathcal{L}_\infty$ and thus $\nu(t)$ and $\dot{z}_1(t)$ are bounded. In view of (3.30)–(3.33), $\hat{\theta}(t), \hat{E}(t), \hat{D}_\ell(t), \hat{F}_\ell(t), \ell = 1, .., h$ are bounded thus $\tau(t)$ in (3.24) is bounded. These boundedness statements are used along with (3.23) to prove $\dot{z}_2(t) \in \mathcal{L}_\infty$. Integrating (3.48) in time guarantees $z_1(t), z_2(t) \in \mathcal{L}_2$. Since $z_1(t), z_2(t) \in \mathcal{L}_2$ and $z_1(t), z_2(t), \dot{z}_1(t), \dot{z}_2(t) \in \mathcal{L}_\infty$, from Barbalat's Lemma (Khalil, 2002), the convergence result in (3.37) is ensured.

3.4. Numerical Simulation Results

To validate the performance of the proposed adaptive controller along with the periodic disturbance estimation method, numerical simulations were conducted for tra-

jectory tracking problem of a ship model. The parameters of the inertia and damping matrices in the ship model in (3.2) are taken from (Fossen and Grovlen, 1998) as

$$M = \begin{bmatrix} 1.0852 & 0 & 0 \\ 0 & 2.0575 & -0.4087 \\ 0 & -0.4087 & 0.2153 \end{bmatrix}, D = \begin{bmatrix} 0.08656 & 0 & 0 \\ 0 & 0.0762 & 0.1510 \\ 0 & 0.0151 & 0.0031 \end{bmatrix} \tag{3.50}$$

and the system was considered to be perturbed by sinusoidal disturbance of the form

$$\tau_d(t) = \begin{bmatrix} \sin(t) \\ \sin(t) \\ \sin(t) \end{bmatrix}. \tag{3.51}$$

The desired trajectory was selected as

$$\eta_d = \begin{bmatrix} 10\sin(0.2t)(1-\exp(-0.3t^3))[m] \\ 10\cos(0.2t)(1-\exp(-0.3t^3))[m] \\ 5\sin(0.2t)(1-\exp(-0.3t^3))[\text{deg}] \end{bmatrix} \tag{3.52}$$

while the initial positions were adjusted as $\eta(0) = [\ 1 \quad -1 \quad 1\ ]^T$ and the initial velocities were set to zero. Several numerical simulations were conducted for different values of harmonic limit h. The controller gains were adjusted to

$$\begin{aligned} K_1 &= \text{diag}\{\ 1.75 \quad 1.75 \quad 1.75\ \} \\ K_2 &= \text{diag}\{\ 15.01 \quad 15.01 \quad 15.01\ \} \\ \Gamma &= 10I_9 \\ \varphi &= 10I_3 \\ \varphi_\ell &= 10I_3,\ \ell = 1, .., h. \end{aligned} \tag{3.53}$$

The results for $h = 3$ are presented in Figures 3.2–3.7. Figures 3.2 illustrates the position tracking error $z_1(t)$. Comparison of the entries of actual position $\eta(t)$ and desired position $\eta_d(t)$ is shown in Figure 3.3 while the actual and desired position presented in xy plane is displayed in Figure 3.4. Figures 3.5 and 3.6 present the auxiliary error $z_2(t)$ and the input

torque $\tau(t)$, respectively while the entries of the parameter estimate vector are presented in Figure 3.7. From Figure 3.2, it is clear that the tracking objective is met.

Additionally, for $h = 0, 1, 3, 5$, simulations were run and $\mathcal{L}_2$ norms and maximum values of the entries of z_1 were evaluated and presented in Table 3.1. In all of these numerical simulations, the tracking control objective was met. From the results given in Table 3.1, it is clear that as h increases, the $\mathcal{L}_2$ norm of the entries of the tracking error decreases.

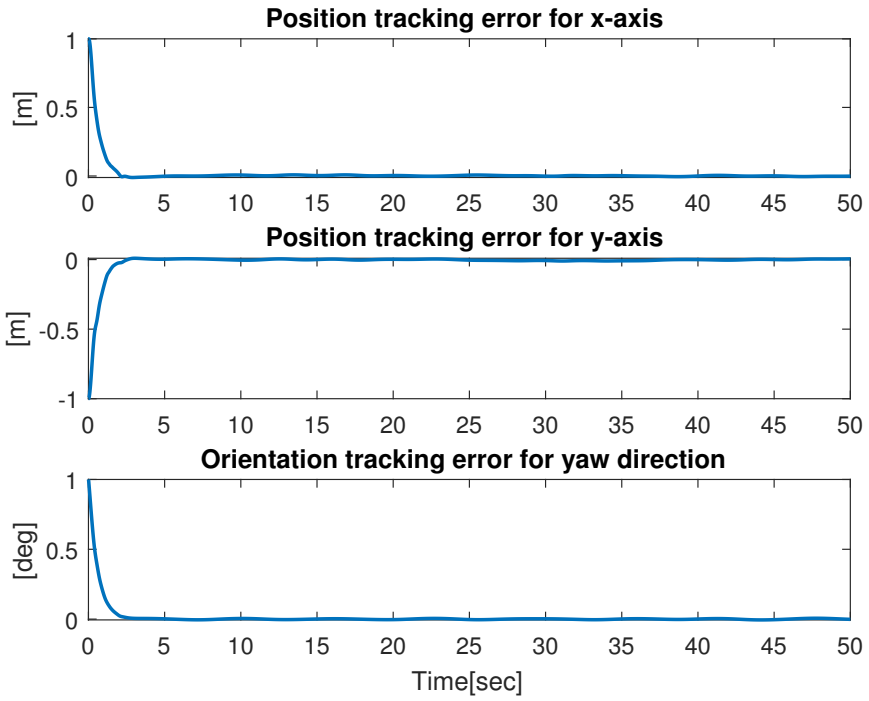

Figure 3.2. Position tracking error $z_1(t)$.

3.5. Evaluation of the Method

In this chapter, a robust adaptive control design supported with periodic disturbance estimation method was utilized for position tracking control of unmanned surface vessels. Backstepping control was utilized in the control design while the disturbance estimation was realized via a Fourier series expansion like method. Lyapunov based arguments were utilized to prove that the designed controller guarantees the convergence of the tracking error in the presence of parametric uncertainties and unknown periodic external disturbances. The presented theoretical results were supported with simulation

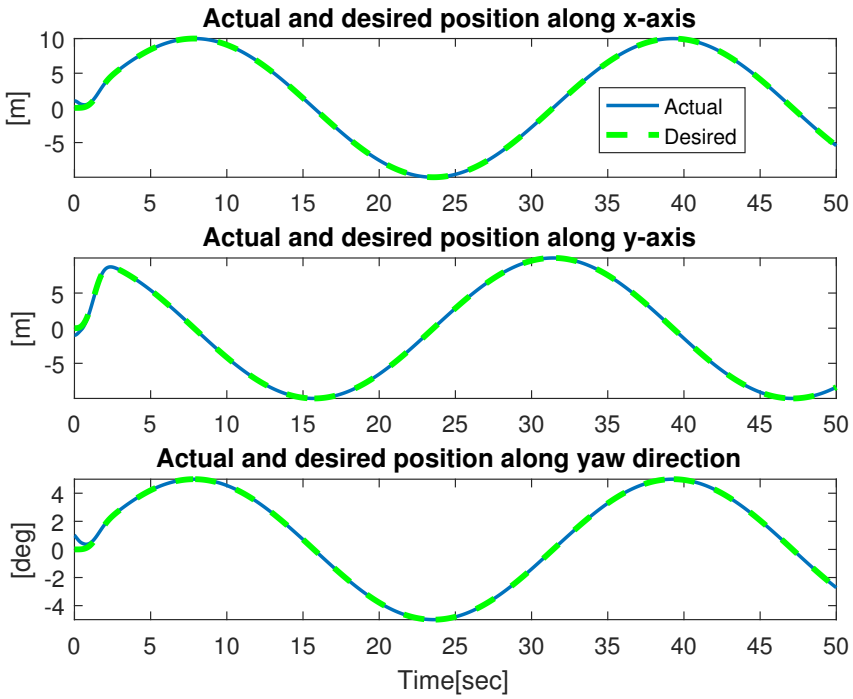

Figure 3.3. Comparison of the actual position $\eta(t)$ and the desired position $\eta_d(t)$.

studies. In these studies, the system was considered to be disturbed by sinusoidal perturbations in (3.51). Different simulation studies were conducted for different values of harmonic limit and it was observed that the designed controller can be efficiently used to meet the control objectives.

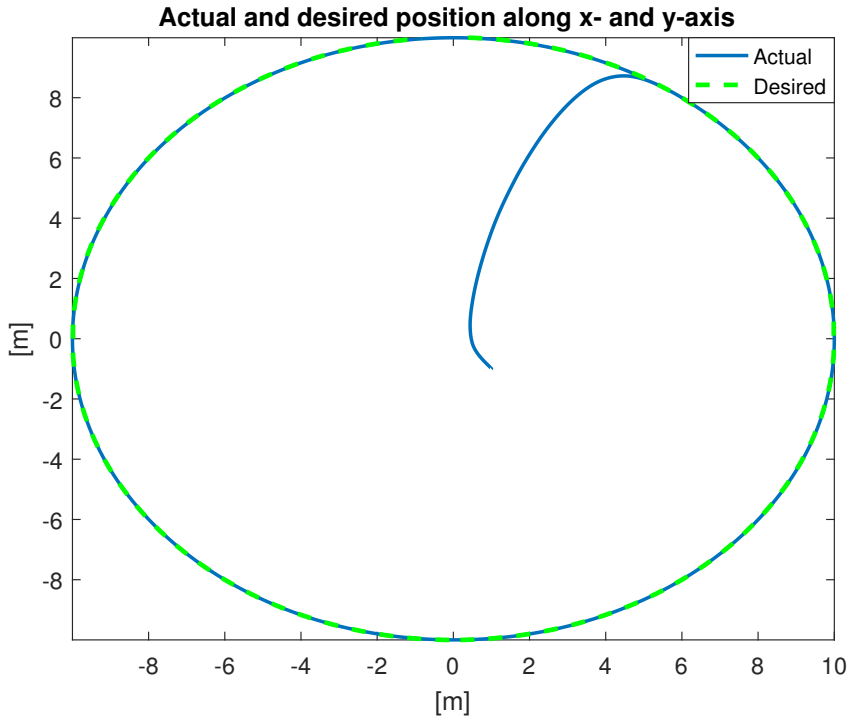

Figure 3.4. Actual position $\eta(t)$ and desired position $\eta_d(t)$ presented in xy plane.

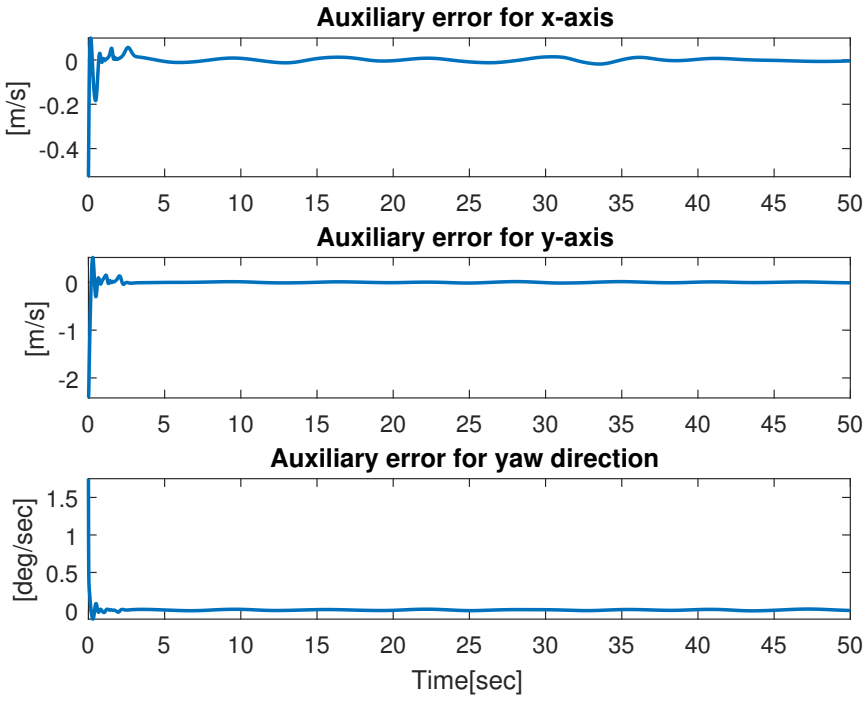

Figure 3.5. Auxiliary error $z_2(t)$.

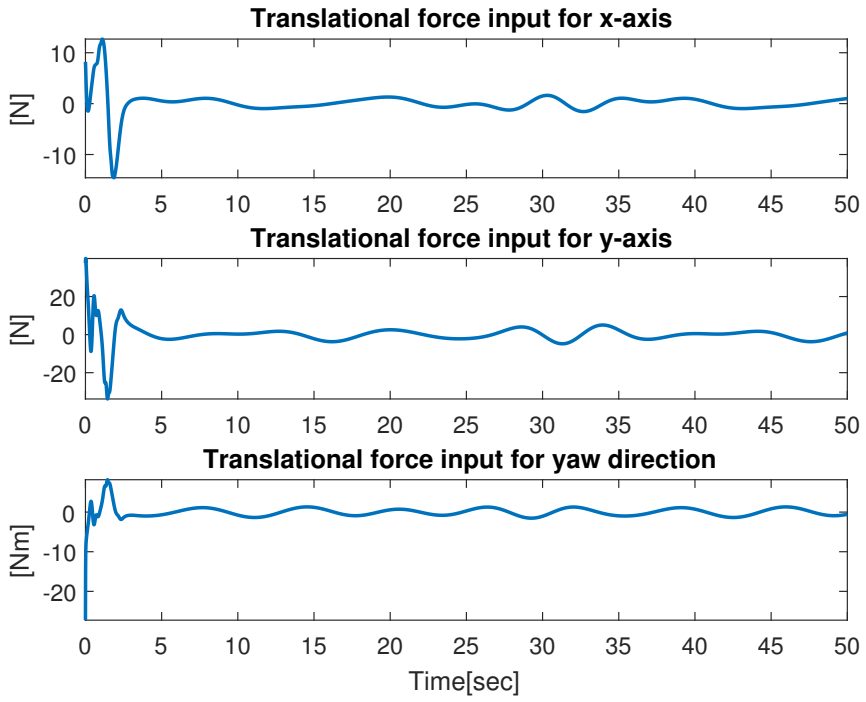

Figure 3.6. Control input torque $\tau(t)$.

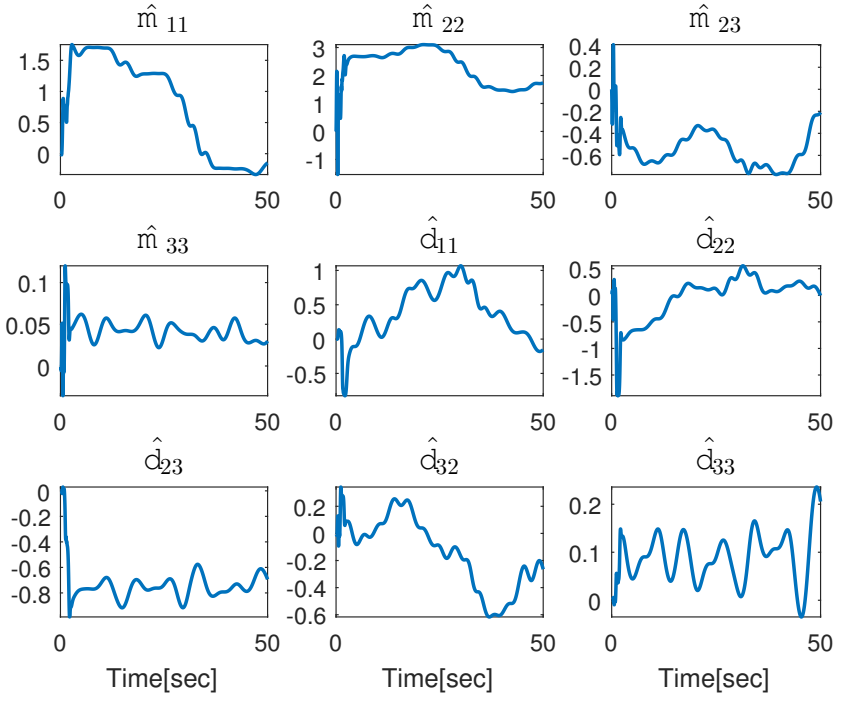

Figure 3.7. Estimations of the entries of M and D matrices.

Table 3.1. Comparison table for different harmonic limits of the approximation.

Harmonic Limit	**States**	**max value of** z_1	$\mathcal{L}_2$ **norm of** z_1	**max**$\lvert\tau_i(t)\rvert$
$h = 0$	Linear position x	1.0030	0.6720	12.8266
	Linear position y	0.2575	0.7613	38.0131
	Yaw angle ψ	1	0.5644	8.0638
$h = 1$	Linear position x	1.0030	0.6530	12.8019
	Linear position y	0.1259	0.6963	38.7162
	Yaw angle ψ	1	0.5594	8.1577
$h = 3$	Linear position x	1.0029	0.6454	12.6860
	Linear position y	0.0633	0.6779	39.9905
	Yaw angle ψ	1	0.5564	8.1688
$h = 5$	Linear position x	1.0029	0.6427	12.6138
	Linear position y	0.0294	0.6692	41.7399
	Yaw angle ψ	1	0.5548	8.0400

CHAPTER 4

OUTPUT FEEDBACK APPROACH

This chapter[1] concentrates on output feedback trajectory tracking control of marine vehicles with dynamical uncertainties. The system under consideration, due to the natural response of oceanic waves, is again considered to be subject to periodic external disturbances. The output feedback structure of the proposed controller algorithm is established via a novel nonlinear model free observer in conjunction with a Fourier series expansion like periodic disturbance estimator. Lyapunov based arguments have been utilized in order to prove the stability of the closed–loop system and the convergence of the tracking and unmeasured state observation errors. Performance demonstration and viability of the proposed method are realized via numerical simulations.

This chapter is organized as follows: Dynamic model of the ship and problem formulation along with error system development are given in Sections 4.1 and 4.2, respectively. Observer–controller design is explained in Section 4.3 while Lyapunov type stability is represented in Section 4.4. Sections 4.5 and 4.6 contain numerical simulation results and conclusions, respectively.

4.1. System Model and Properties

In this section, the dynamic model of the marine vessel will be given which after some straightforward mathematical manipulations will be put in a robot manipulator dynamic model like form along with some important properties that will be utilized in the rest of the derivations. The mathematical model for the dynamically positioned ship is considered to be of the following form (Fossen, 2002)

[1]For the completeness and compactness of this chapter, some definitions and model properties are repeated.

$$\dot{\eta} = R\nu \tag{4.1}$$

$$M\dot{\nu} + D\nu + d = \tau \tag{4.2}$$

where $\eta(t)$, $\nu(t) \in \mathbb{R}^3$ represent the position and the velocity of the ship, respectively, $M \in \mathbb{R}^{3\times3}$ is the constant, positive definite, symmetric, mass inertia matrix, $D \in \mathbb{R}^{3\times3}$ is the constant, damping matrix, $d(t) \in \mathbb{R}^3$ is additive, periodic disturbances, $\tau(t) \in \mathbb{R}^3$ is the control input, and $R(\psi) \in SO(3)$ represents the orthogonal rotation matrix between the Earth and body–fixed coordinate frames. The position and velocity vectors are in the form $\eta \triangleq [\ x(t) \quad y(t) \quad \psi(t)\ ]^T$ and $\nu = [\ \nu_u(t) \quad \nu_v(t) \quad \nu_r(t)\ ]^T$, respectively, where $x(t)$, $y(t) \in \mathbb{R}$ denote the translational positions, $\psi(t) \in \mathbb{R}$ is the rotation about yaw axes of the ship, while $\nu_u(t)$, $\nu_v(t) \in \mathbb{R}$ represent the translational velocities and $\nu_r(t) \in \mathbb{R}$ is the rotational velocity about the yaw axes. The above mentioned system matrices have following structural forms

$$M = \begin{bmatrix} m_{11} & 0 & 0 \\ 0 & m_{22} & m_{23} \\ 0 & m_{23} & m_{33} \end{bmatrix}, D = \begin{bmatrix} d_{11} & 0 & 0 \\ 0 & d_{22} & d_{23} \\ 0 & d_{32} & d_{33} \end{bmatrix} \tag{4.3}$$

where their entries are constant and rotation matrix $R(\psi)$ has the form

$$R(\psi) = \begin{bmatrix} \cos(\psi) & -\sin(\psi) & 0 \\ \sin(\psi) & \cos(\psi) & 0 \\ 0 & 0 & 1 \end{bmatrix}. \tag{4.4}$$

After substituting (4.1) and its time derivative into (4.2) and making use of $R^{-1} = R^T$, a compact representation of the mathematical model of the marine vessel can be obtained as

$$J\ddot{\eta} + C\dot{\eta} + F\dot{\eta} + \tau_d = \tau^* \tag{4.5}$$

where $J(\eta)$, $C(\eta, \dot{\eta})$, $F(\eta) \in \mathbb{R}^{3\times3}$ and the control input $\tau^*(t) \in \mathbb{R}^3$ are defined as

$$J \triangleq RMR^T,\ C \triangleq RM\dot{R}^T,\ F \triangleq RDR^T,\ \tau_d \triangleq Rd,\ \tau^* \triangleq R\tau. \tag{4.6}$$

The compact model in (4.5) is sometimes referred to as robot–like model due to its presentation being similar to standard robot manipulator dynamic models. The dynamic model given by (4.5) satisfies the following standard model properties.

Property 1 *The matrix $J(\eta)$ is symmetric, positive definite and has lower and upper bounds as (Fossen, 2002)*

$$m_l I_3 \leq J \leq m_u I_3 \tag{4.7}$$

where m_l and m_u are known, positive constants and $I_3 \in \mathbb{R}^{3\times 3}$ is the standard identity matrix. Likewise, $J^{-1}(\eta)$ satisfies below inequalities

$$\frac{1}{m_u} I_3 \leq J^{-1} \leq \frac{1}{m_l} I_3. \tag{4.8}$$

Property 2 *The matrices $J(\eta)$ and $C(\eta, \dot{\eta})$ satisfy the given skew–symmetry relationship (Fossen, 2002)*

$$\xi^T \left(\frac{1}{2} \dot{J}(\eta) - C(\eta, \dot{\eta}) \right) \xi = 0 \; \forall \xi \in \mathbb{R}^3. \tag{4.9}$$

Property 3 *The dynamic term $C(\eta, \dot{\eta})$ has the given relationship*

$$C(\vartheta, \varrho)\kappa = C(\vartheta, \kappa)\varrho \; \forall \vartheta, \varrho, \kappa \in \mathbb{R}^3. \tag{4.10}$$

Property 4 *The dynamics terms $J(\eta), C(\eta, \dot{\eta}), F(\eta)$ have following upper bounds*

$$\begin{aligned}
\left\| J(\vartheta) - J(\varrho) \right\|_{i\infty} &\leq \zeta_{j1} \|\vartheta - \varrho\| && (4.11)\\
\left\| J^{-1}(\vartheta) - J^{-1}(\varrho) \right\|_{i\infty} &\leq \zeta_{j2} \|\vartheta - \varrho\| && (4.12)\\
\left\| C(\vartheta, \varrho) \right\|_{i\infty} &\leq \zeta_{c1} \|\varrho\| && (4.13)\\
\left\| C(\vartheta, \varrho) - C(\kappa, \varrho) \right\|_{i\infty} &\leq \zeta_{c2} \|\varrho\| \|\vartheta - \kappa\| && (4.14)\\
\left\| F(\vartheta) \right\|_{i\infty} &\leq \zeta_{f1} && (4.15)\\
\left\| F(\vartheta) - F(\varrho) \right\|_{i\infty} &\leq \zeta_{f2} \|\vartheta - \varrho\| && (4.16)
\end{aligned}$$

where $\vartheta, \varrho, \kappa \in \mathbb{R}^3$, $\zeta_{j1}, \zeta_{j2}, \zeta_{c1}, \zeta_{c2}, \zeta_{f1}, \zeta_{f2} \in \mathbb{R}$ are positive constants and $\left\| (\cdot) \right\|_{i\infty}$ is the induced infinity norm.

Property 5 *The left hand side of* (4.5) *can be partitioned as (Aksoy et al., 2017)*

$$J(\eta)\ddot{\eta} + C(\eta,\dot{\eta})\dot{\eta} + F(\eta)\dot{\eta} + \tau_d = Y(\eta,\dot{\eta},\ddot{\eta})\theta + \gamma \tag{4.17}$$

where $Y(\eta,\dot{\eta},\ddot{\eta}) \in \mathbb{R}^{3\times 9}$ *denotes the regression matrix,* $\theta \in \mathbb{R}^9$ *is a constant vector containing system parameters introduced in* (4.3) *and is defined as*

$$\theta \triangleq [\ m_{11} \quad m_{22} \quad m_{23} \quad m_{33} \quad d_{11} \quad d_{22} \quad d_{23} \quad d_{32} \quad d_{33}\ ]^T \tag{4.18}$$

and $\gamma(t) \in \mathbb{R}^3$ *includes periodic disturbance effects. Additionally desired version of* (4.17) *can be introduced as*

$$J(\eta_d)\ddot{\eta}_d + C(\eta_d,\dot{\eta}_d)\dot{\eta}_d + F(\eta_d)\dot{\eta}_d + \tau_d = Y_d(\eta_d,\dot{\eta}_d,\ddot{\eta}_d)\theta + \gamma \tag{4.19}$$

in which $Y_d(\eta_d,\dot{\eta}_d,\ddot{\eta}_d) \in \mathbb{R}^{3\times 9}$ *is a function of the desired position* $\eta_d(t) \in \mathbb{R}^3$ *and its time derivatives while the remaining terms are same as in* (4.17)*.*

4.2. Problem Formulation and Error System Development

In this section, the control problem along with the model constraints and also the error system development will be presented. The main control objective is to ensure that the position vector will track desired position vector despite anomalies in the mathematical model of the marine vessel. Specifically, the mathematical model in (4.2) (and thus its compact form in (4.5)) is uncertain due to presence of uncertain model parameters (*i.e.*, θ in (4.17) or (4.19) is unknown) and also due to the periodic disturbance vector d. The control problem is further complicated by the velocity vector $\nu(t)$ being unavailable for control design. The subsequent development requires the desired trajectory to be designed as sufficiently smooth.

To quantify the main control objective, a tracking error, denoted by $e(t) \in \mathbb{R}^3$, is defined as

$$e \triangleq \eta_d - \eta. \tag{4.20}$$

To deal with the restriction of velocity measurements being unavailable, in this chapter, an observer based strategy will be employed. Specifically, a velocity observer, denoted by $\dot{\hat{\eta}}(t) \in \mathbb{R}^3$, will be introduced in the subsequent sections and to quantify the observation error, velocity observation error, shown with $\dot{\tilde{\eta}}(t) \in \mathbb{R}^3$, and the corresponding position observation error, represented by $\tilde{\eta}(t) \in \mathbb{R}^3$, are defined in the following manner

$$\dot{\tilde{\eta}} \triangleq \dot{\eta} - \dot{\hat{\eta}} \tag{4.21}$$

$$\tilde{\eta} \triangleq \eta - \hat{\eta} \tag{4.22}$$

where $\hat{\eta}(t) \in \mathbb{R}^3$ is the observed position.

To ease the presentation of the subsequent design and, at the same time, to have only first time derivatives in the accompanying stability analysis, two auxiliary errors, namely filtered position tracking error $r(t) \in \mathbb{R}^3$ and filtered velocity observation error $s(t) \in \mathbb{R}^3$, are introduced

$$r \triangleq \dot{e} + \mu e \tag{4.23}$$

$$s \triangleq \dot{\tilde{\eta}} + \mu \tilde{\eta} \tag{4.24}$$

with $\mu \in \mathbb{R}$ being a constant, positive gain. It is easy to notice that due to the need of $\dot{\eta}$ for them to be computed, neither $r(t)$ nor $s(t)$ are available. However, it is easy practice to show that

$$r + s = \dot{\eta}_d - \dot{\hat{\eta}} + \mu(\eta_d - \hat{\eta}) \tag{4.25}$$

where all the signals at the right hand side being available.

Following property imposed on the periodic perturbation introduced in Property 5 is essential for the subsequent development.

Property 6 *The periodic disturbance term $\gamma(t)$ can be modeled as (Aksoy et al., 2017)*

$$\gamma = E^T \mathit{Tanh}(e) + \sum_{\ell=1}^{h} D_\ell^T \mathit{Sin}(\ell e) \tag{4.26}$$

in which $h \in \mathbb{R}^{+}$ *represents the harmonic limit and* $E = diag\{\ E_1 \quad E_2 \quad E_3\ \}$, $D_\ell = diag\{\ D_{\ell 1} \quad D_{\ell 2} \quad D_{\ell 3}\ \} \in \mathbb{R}^{3\times 3}$, $\ell = 1, \cdots, h$ *are unknown, constant, diagonal matrices standing for the mean value of the disturbance weights and contributions of different error frequencies, respectively, and*

$$\textit{Tanh}\,(e) = [\ \tanh(e_1) \quad \tanh(e_2) \quad \tanh(e_3)\ ]^T \tag{4.27}$$

$$\textit{Sin}\,(\ell e) = [\ \sin(\ell e_1) \quad \sin(\ell e_2) \quad \sin(\ell e_3)\ ]^T \tag{4.28}$$

for $e = [\ e_1 \quad e_2 \quad e_3\ ]^T$.

4.3. Observer–Controller Couple Design

In this section, the velocity observer and the control input fused with periodic disturbance estimation component will be designed, and the closed–loop error systems for both tracking error and velocity observation will be obtained.

4.3.1. Controller Design

Based on the subsequent stability analysis, the control input τ^* is designed as follows

$$\tau^* = Y_d\hat{\theta} + K_p e + K_c\left(\dot{\eta}_d - \dot{\hat{\eta}}\right) + \mu K_c\left(\eta_d - \hat{\eta}\right) + \hat{E}^T \text{Tanh}\,(e) + \sum_{\ell=1}^{h} \hat{D}_\ell^T \text{Sin}\,(\ell e) \tag{4.29}$$

where $\hat{\theta}(t) \in \mathbb{R}^9$, $\hat{E}(t) \in \mathbb{R}^{3\times 3}$ and $\hat{D}_\ell(t) \in \mathbb{R}^{3\times 3}$ stand for the estimates of θ, E and D_ℓ, respectively, and are updated adaptively as

$$\begin{aligned}\hat{\theta}(t) = \text{Proj}\Bigg\{&\Gamma\int_0^t \left[\mu Y_d^T(\sigma)\, e(\sigma) - \frac{dY_d^T(\sigma)}{d\sigma} e(\sigma)\right] d\sigma \\ &+\Gamma\left[Y_d^T(t)\, e(t) - Y_d^T(0)\, e(0)\right]\Bigg\}\end{aligned} \tag{4.30}$$

$$\hat{E}(t) = \Psi\int_0^t \mu d_e(\sigma)\, d_{\tanh}(\sigma)\, d\sigma + \Psi d_{\ln}(t) - \Psi d_{\ln}(0) \tag{4.31}$$

$$\hat{D}_\ell(t) = \Psi_\ell\int_0^t \mu d_e(\sigma)\, d_{\sin}(\sigma)\, d\sigma - \frac{1}{\ell}\Psi_\ell d_{\cos}(t) + \frac{1}{\ell}\Psi_\ell d_{\cos}(0) \tag{4.32}$$

in which Proj : $\mathbb{R}^9 \to \mathbb{R}^9$ is a projection operator[2], $\Gamma \in \mathbb{R}^{9\times 9}$, $\Psi \in \mathbb{R}^{3\times 3}$, $\Psi_\ell \in \mathbb{R}^{3\times 3}$ for $\ell = 1, \cdots, h$ are constant, diagonal, positive definite adaptation gain matrices, $d_e(t)$, $d_{\tanh}(t)$, $d_{\cos}(t)$, $d_{\sin}(t)$, $d_{\ln}(t) \in \mathbb{R}^{3\times 3}$ are defined as

$$d_e \triangleq \text{diag}\{\ e_1 \quad e_2 \quad e_3\ \} \tag{4.33}$$

$$d_{\tanh} \triangleq \text{diag}\{\ \tanh(e_1) \quad \tanh(e_2) \quad \tanh(e_3)\ \} \tag{4.34}$$

$$d_{\cos} \triangleq \text{diag}\{\ \cos(\ell e_1) \quad \cos(\ell e_2) \quad \cos(\ell e_3)\ \} \tag{4.35}$$

$$d_{\sin} \triangleq \text{diag}\{\ \sin(\ell e_1) \quad \sin(\ell e_2) \quad \sin(\ell e_3)\ \} \tag{4.36}$$

$$d_{\ln} \triangleq \text{diag}\{\ \ln\big(\cosh(\ell e_1)\big) \quad \ln\big(\cosh(\ell e_2)\big) \quad \ln\big(\cosh(\ell e_3)\big)\ \}. \tag{4.37}$$

The flow diagram of the controller in (4.29) is given in Figure 4.1.

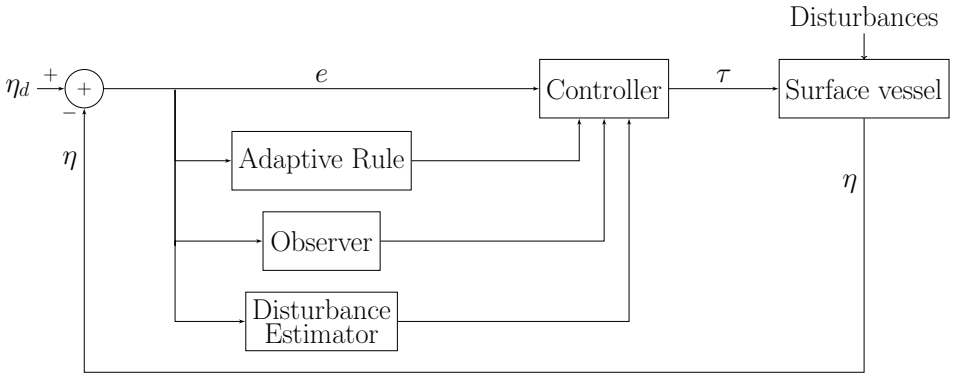

Figure 4.1. Flow diagram of the OFB controller in (4.29).

The terms in the control input design in (4.29) are now briefly discussed. The terms $K_p e + K_c(\dot{\eta}_d - \dot{\hat{\eta}}) + \mu K_c(\eta_d - \hat{\eta})$ are feedback components. The adaptive term $Y_d\hat{\theta}$ is designed to compensate for uncertain model parameters adaptively while the other terms are for estimating the uncertain periodic disturbances. After premultiplying time derivative of (4.23) with $J(\eta)$, utilizing (4.5) and (4.23), dynamics of $r(t)$ is found as

$$J\dot{r} = -Cr + Y_s\theta + \gamma - \tau^* \tag{4.38}$$

where $Y_s(e, \dot{e}, \eta_d, \dot{\eta}_d, \ddot{\eta}_d) \in \mathbb{R}^{3\times 9}$ is a regressor matrix obtained from

[2]In (4.30), the projection algorithm is used to ensure the boundedness of $\hat{\theta}(t)$ and its time derivative since required by the subsequent stability analysis.

$$Y_s\theta + \gamma = J(\eta)\left(\ddot{\eta}_d + \mu\dot{e}\right) + C(\eta,\dot{\eta})\left(\dot{\eta}_d + \mu e\right) + F(\eta)\dot{\eta} + \tau_d. \tag{4.39}$$

Substituting the control input in (4.29) into (4.38) yields the following closed–loop error dynamics for $r\left(t\right)$

$$J\dot{r} = -Cr + \chi - K_p e - K_c\left(r+s\right) + Y_d\tilde{\theta} + \tilde{E}\text{Tanh}\left(e\right) + \sum_{\ell=1}^{h}\tilde{D}_\ell\text{Sin}\left(\ell e\right) \tag{4.40}$$

in which $\tilde{\theta}\left(t\right) \in \mathbb{R}^9$, $\tilde{E}\left(t\right) \in \mathbb{R}^{3\times3}$, $\tilde{D}_\ell\left(t\right) \in \mathbb{R}^{3\times3}$ are parameter estimation errors defined as

$$\tilde{\theta} \triangleq \theta - \hat{\theta} \tag{4.41}$$

$$\tilde{E} \triangleq E - \hat{E} \tag{4.42}$$

$$\tilde{D}_\ell \triangleq D_\ell - \hat{D}_\ell \tag{4.43}$$

and $\chi\left(t\right) \in \mathbb{R}^3$ is an auxiliary term defined as

$$\chi \triangleq Y_s\theta - Y_d\theta \tag{4.44}$$

which can be upper bounded as

$$\|\chi\| \leq \rho_1\|e\| + \rho_2\|r\| \tag{4.45}$$

where $\rho_1\left(\|e\|\right)$, $\rho_2\left(\|e\|\right) \in \mathbb{R}$ being known, positive bounding functions. In Appendix A, the bound of $\left\|\chi(t)\right\|$ in (4.45) is presented.

4.3.2. Observer Design

The velocity observer is updated according to

$$\dot{\hat{\eta}} = p + K_0\tilde{\eta} - K_c e \tag{4.46}$$

$$\dot{p} = K_1\text{Sgn}\left(\tilde{\eta}\right) + K_2\tilde{\eta} - \mu K_c e \tag{4.47}$$

in which $p(t) \in \mathbb{R}^3$ is an auxiliary filter vector, $\text{Sgn}(\tilde{\eta}) \in \mathbb{R}^3$ is the vector form of the signum function, and K_0, K_1, K_2, $K_c \in \mathbb{R}^{3\times 3}$ are constant, diagonal, positive definite gain matrices. Substituting (4.47) into the time derivative of (4.46) results in

$$\dot{\tilde{\eta}} = K_1 \text{Sgn}(\tilde{\eta}) + K_2\tilde{\eta} + K_0\dot{\tilde{\eta}} - K_c r \tag{4.48}$$

where (4.23) was made use of as well. By utilizing (4.5) and (4.48), the time derivative of (4.21) is obtained as

$$\ddot{\tilde{\eta}} = N - K_1 \text{Sgn}(\tilde{\eta}) - K_2\tilde{\eta} - K_0\dot{\tilde{\eta}} + K_c r \tag{4.49}$$

where $N(t) \in \mathbb{R}^3$ is defined as

$$N \triangleq J^{-1}\left(\tau^* - C\dot{\eta} - F\dot{\eta} - \tau_d\right) \tag{4.50}$$

which can be separated as sum of two terms

$$N = N_d + N_b \tag{4.51}$$

with $N_d(t)$, $N_b(t) \in \mathbb{R}^3$ being defined as

$$N_d \triangleq \ddot{\eta}_d - J^{-1}(\eta_d) Y_d \tilde{\theta} \tag{4.52}$$

$$\begin{aligned} N_b \triangleq\ & \left[J^{-1}(\eta_d) - J^{-1}(\eta)\right]\left(Y_d\tilde{\theta} - J(\eta_d)\ddot{\eta}_d\right) \\ & + J^{-1}(\eta)\left[K_p e + K_c(r+s) - \tilde{E}\text{Tanh}(e) - \sum_{\ell=1}^{h}\tilde{D}_\ell \text{Sin}(\ell e)\right] \\ & + J^{-1}(\eta)\left[C(\eta_d,\dot{\eta}_d)\dot{\eta}_d - C(\eta,\dot{\eta})\dot{\eta} + F(\eta_d)\dot{\eta}_d - F(\eta)\dot{\eta}\right]. \end{aligned} \tag{4.53}$$

Utilizing the fact that desired trajectory is sufficiently smooth, Property 1 and the output of the projection operator being bounded yield $N_d(t)$ and its time derivative can be proven to be bounded. Based on its structure in (4.53), $N_b(t)$ can be shown to be upper bounded as

$$\|N_b\| \leq \rho_{01}\|e\| + \rho_{02}\|r\| + \rho_{03}\|e\|\|r\| + \rho_{04}\|r\|^2 + \rho_{05}\|s\| \tag{4.54}$$

where ρ_{01}, ρ_{02}, ρ_{03}, ρ_{04}, ρ_{05} are known, positive bounding constants. In Appendix A, the bound of $\left\|N_b(t)\right\|$ in (4.54) is presented.

After substituting (4.49) into the time derivative of (4.24) and utilizing (4.51)–(4.53), dynamics for $s\left(t\right)$ is found as

$$\dot{s} = N_d + N_b - K_1 \text{Sgn}\left(\tilde{\eta}\right) - K_2\tilde{\eta} - K_0\dot{\tilde{\eta}} + K_c r + \mu\dot{\tilde{\eta}} \tag{4.55}$$

and selecting the gains μ, K_0 and K_2 to satisfy

$$\mu\left(K_0 - \mu I_3\right) = K_2 \tag{4.56}$$

then following form is reached

$$\dot{s} = N_d + N_b - K_1 \text{Sgn}\left(\tilde{\eta}\right) - \frac{1}{\mu}K_2 s + K_c r. \tag{4.57}$$

4.4. Stability Analysis

The stability of the closed–loop system under the designed observer–controller couple is analyzed.

Theorem 4.4.1 *The velocity observer design in* (4.46)–(4.47)*, the control input in* (4.29) *in conjunction with the adaptive update rule in* (4.30) *and the estimation of the periodic disturbance parameters in* (4.31)–(4.32) *ensures asymptotic stability in the sense that*

$$\|e\left(t\right)\|, \|\dot{\tilde{\eta}}\left(t\right)\| \to 0 \text{ as } t \to \infty \tag{4.58}$$

provided that the observer gain is selected to satisfy (4.56)*,* $\mu\lambda_{\min}\{K_p\} \geq 1$ *is ensured, and* K_c *and* K_2 *are designed as*

$$K_c = \left(1 + \rho_2 + k_n\rho_1^2\right) I_3 \tag{4.59}$$

$$K_2 = \mu\left(1 + \rho_{05} + k_n\left(\rho_{01}^2 + \rho_{02}^2 + \rho_{03}^2 + \rho_{04}^2\right)\right) I_3 \tag{4.60}$$

with $k_n \in \mathbb{R}$ being a nonlinear damping gain chosen to satisfy the following inequality

$$k_n > \frac{1}{2}\left(1 + \frac{\lambda_2}{2\lambda_1}\|z(0)\|^2\right) \tag{4.61}$$

in which positive bounding constants λ_1, $\lambda_2 \in \mathbb{R}$ and combined error vector $z(t) \in \mathbb{R}^{(22+3h)\times 1}$ are defined as

$$\lambda_1 \triangleq \frac{1}{2}\min\{1, m_1, \lambda_{\min}\{K_p\}, \lambda_{\min}\{\Gamma^{-1}\}, \lambda_{\min}\{\Psi^{-1}\}, \lambda_{\min}\{\Psi_\ell^{-1}\}\} \tag{4.62}$$

$$\lambda_2 \triangleq \frac{1}{2}\max\{2, m_2, \lambda_{\max}\{K_p\}, \lambda_{\max}\{\Gamma^{-1}\}, \lambda_{\max}\{\Psi^{-1}\}, \lambda_{\max}\{\Psi_\ell^{-1}\}\} \tag{4.63}$$

$$z \triangleq \begin{bmatrix} s^T & r^T & e^T & \sqrt{P} & \tilde{\theta}^T & \upsilon_{\tilde{E}}^T & \upsilon_{\tilde{D}_\ell}^T \end{bmatrix}^T \tag{4.64}$$

where $\upsilon_{\tilde{E}}(t) \in \mathbb{R}^3$ and $\upsilon_{\tilde{D}_\ell}(t) \in \mathbb{R}^{3h}$ are defined as

$$\upsilon_{\tilde{E}} \triangleq \begin{bmatrix} \tilde{E}_1 & \tilde{E}_2 & \tilde{E}_3 \end{bmatrix}^T \tag{4.65}$$

$$\upsilon_{\tilde{D}_\ell} \triangleq \begin{bmatrix} \tilde{D}_{11} & \tilde{D}_{12} & \tilde{D}_{13} & \cdots & \tilde{D}_{h1} & \tilde{D}_{h2} & \tilde{D}_{h3} \end{bmatrix}^T. \tag{4.66}$$

Proof To prove the theorem, a non–negative Lyapunov function, denoted by $V(t) \in \mathbb{R}$, is defined as

$$\begin{aligned} V \triangleq\ & \frac{1}{2}s^T s + P + \frac{1}{2}r^T J r + \frac{1}{2}e^T K_p e + \frac{1}{2}\tilde{\theta}^T \Gamma^{-1}\tilde{\theta} \\ & + \frac{1}{2}\text{tr}\{\tilde{E}^T \Psi^{-1}\tilde{E}\} + \frac{1}{2}\text{tr}\left\{\sum_{\ell=1}^{h} \tilde{D}_\ell \Psi_\ell^{-1}\tilde{D}_\ell\right\} \end{aligned} \tag{4.67}$$

where $\text{tr}\{\cdot\}$ is the trace operation and $P(t) \in \mathbb{R}$ is defined as

$$P \triangleq \zeta_0 - \int_0^t w_0(\sigma)\, d\sigma \tag{4.68}$$

in which $w_0(t)$, $\zeta_0 \in \mathbb{R}$ are defined as[3]

[3]Subscript i represents the ith entry of a column vector or the ith diagonal entry of a matrix.

$$w_0 \triangleq s^T \left(N_d - K_1 \text{Sgn}\left(\tilde{\eta}\right)\right) \tag{4.69}$$

$$\zeta_0 \triangleq \sum_{i=1}^{3} K_{1i} |\tilde{\eta}_i\left(0\right)| - \tilde{\eta}^T\left(0\right) N_d\left(0\right). \tag{4.70}$$

If the entries of K_1 are selected to satisfy following constraint

$$K_{1i} \geq |N_{di}\left(t\right)| + \frac{1}{\mu} |\dot{N}_{di}\left(t\right)| \; \forall t \in \mathbb{R}, i = 1, 2, 3 \tag{4.71}$$

then $P\left(t\right)$ is non–negative (Xian et al., 2004), (Zergeroglu et al., 2017). Therefore, $V\left(t\right)$ is a Lyapunov function and can be upper and lower bounded as

$$\lambda_1 \|q\|^2 \leq \lambda_1 \|z\|^2 \leq V \leq \lambda_2 \|z\|^2 \tag{4.72}$$

where $q\left(t\right) \in \mathbb{R}^9$ is defined as

$$q \triangleq \begin{bmatrix} s^T & r^T & e^T \end{bmatrix}^T. \tag{4.73}$$

After taking the time derivative of (4.67), utilizing (4.23), time derivatives of (4.30)–(4.32) and (4.40)–(4.43), (4.57), Property 2, and time derivative of (4.68), $\dot{V}$ is obtained in a more compact form as

$$\dot{V} = s^T \left(N_b - \frac{1}{\mu} K_2 s\right) + r^T \left(\chi - K_c r\right) - \mu e^T K_p e. \tag{4.74}$$

Using the bounds of N_b in (4.54) and χ in (4.45) yields

$$\begin{aligned} \dot{V} \leq & -\|s\|^2 - \|r\|^2 - \mu \lambda_{\min}\{K_p\} \|e\|^2 + \left(\rho_{01} \|s\| \|e\| - k_n \rho_{01}^2 \|s\|^2\right) \\ & + \left(\rho_{02} \|s\| \|r\| - k_n \rho_{02}^2 \|s\|^2\right) + \left(\rho_{03} \|s\| \|r\| \|e\| - k_n \rho_{03}^2 \|s\|^2\right) \\ & + \left(\rho_{04} \|r\|^2 \|s\| - k_n \rho_{04}^2 \|s\|^2\right) + \left(\rho_1 \|r\| \|e\| - k_n \rho_1^2 \|r\|^2\right) \end{aligned} \tag{4.75}$$

and after completing the squares in the bracketed terms it can be restated as

$$\begin{aligned} \dot{V} \leq & -\left(\mu \lambda_{\min}\{K_p\} - \frac{1}{2k_n} - \frac{1}{4k_n} \|r\|^2\right) \|e\|^2 \\ & -\left(1 - \frac{1}{4k_n} - \frac{1}{4k_n} \|r\|^2\right) \|r\|^2 - \|s\|^2. \end{aligned} \tag{4.76}$$

In view of (4.73), a more conservative upper bound of (4.76) can be obtained as

$$\dot{V} \leq -\left[1 - \frac{1}{2k_n}\left(1 + \frac{1}{2}\|q\|^2\right)\right]\|q\|^2 \tag{4.77}$$

and for negativeness of $\dot{V}$, the square bracketed term must satisfy the following condition

$$1 - \frac{1}{2k_n}\left(1 + \frac{1}{2}\|q\|^2\right) > 0 \tag{4.78}$$

which in view of (4.72) can be restated as

$$1 - \frac{1}{2k_n}\left(1 + \frac{V(t)}{2\lambda_1}\right) > 0. \tag{4.79}$$

Thus, the right hand side of (4.77) can be rewritten as

$$\dot{V} \leq -\beta\|q\|^2 \text{ provided that } 2k_n > 1 + \frac{V(t)}{2\lambda_1} \tag{4.80}$$

where $\beta \in \mathbb{R}$ is a positive constant varying between $0 < \beta \leq 1$. A more conservative bound can be obtained as in (4.61) when (4.72) is made use of.

Since $V(t)$ is positive definite and its time derivative is negative, we can conclude that $V(t)$ is bounded thus, from its definition in (4.67), $P(t)$, $e(t)$, $r(t)$, $s(t)$, $\tilde{\theta}(t)$, $\tilde{D}_\ell(t)$, $\tilde{E}(t) \in \mathcal{L}_\infty$. By using standard signal chasing arguments, boundedness of all the signals under the closed–loop system can be proven. After integrating (4.80) in time, $q(t) \in \mathcal{L}_2$, therefore $e(t)$, $\dot{\tilde{\eta}}(t) \in \mathcal{L}_2$ can be proven. Finally by using Barbalat's Lemma (Khalil, 2002), asymptotic convergence of the position tracking error and the velocity observer error to the origin is proven.

4.5. Numerical Simulation Results

To illustrate the performance of the proposed observer–controller couple along with the periodic disturbance estimation method, numerical simulations were performed.

The parameters of the dynamic terms in the ship model (4.2) were selected as (Fossen and Grovlen, 1998)

$$M = \begin{bmatrix} 1.0852 & 0 & 0 \\ 0 & 2.0575 & -0.4087 \\ 0 & -0.4087 & 0.2153 \end{bmatrix}, D = \begin{bmatrix} 0.08656 & 0 & 0 \\ 0 & 0.0762 & 0.1510 \\ 0 & 0.0151 & 0.0031 \end{bmatrix} \tag{4.81}$$

and the system was considered to be disturbed by sinusoidal perturbation of the form

$$d(t) = \begin{bmatrix} \sin(t) \\ \sin(t) \\ \sin(t) \end{bmatrix}. \tag{4.82}$$

The desired position of the ship was chosen as

$$\eta_d = \begin{bmatrix} 10\sin(0.2t)\,[\mathrm{m}] \\ 10\cos(0.2t)\,[\mathrm{m}] \\ 5\sin(0.2t)\,[\mathrm{deg}] \end{bmatrix} \tag{4.83}$$

and the initial position was adjusted as $\eta(0) = \begin{bmatrix} 1\,[\mathrm{m}] & -1\,[\mathrm{m}] & 1\,[\mathrm{deg}] \end{bmatrix}^T$ while the initial velocity was set to zero. Several numerical simulations were conducted for different values of harmonic limit h. The controller–observer gains were adjusted to

$$\begin{aligned} \mu &= 2 \\ \Gamma &= I_9 \\ K_p &= \mathrm{diag}\{\ 2 \quad 1.51 \quad 1.45\ \} \\ K_0 &= \mathrm{diag}\{\ 22 \quad 25 \quad 21\ \} \\ K_1 &= \mathrm{diag}\{\ 20 \quad 25 \quad 21\ \} \\ K_c &= \mathrm{diag}\{\ 2 \quad 5 \quad 2\ \} \\ \Psi &= \mathrm{diag}\{\ 40 \quad 2 \quad 2\ \} \\ \Psi_\ell &= \begin{cases} \mathrm{diag}\{\ 20 \quad 2 \quad 2\ \} & \ell < 5 \\ \mathrm{diag}\{\ 30 \quad 20 \quad 4\ \} & \ell = 5. \end{cases} \end{aligned}$$

The results are shown for $h = 3$ in Figures 4.2–4.9. Figures 4.2 illustrates the position tracking error $e(t)$. Comparison of the entries of actual position $\eta(t)$ and desired position $\eta_d(t)$ is shown in Figure 4.3 while the actual and desired position presented in xy plane is displayed in Figure 4.4. The position observation error $\tilde{\eta}(t)$ is presented in Figure 4.5 while Figures 4.6 and 4.7 show the actual and observed position, respectively. The control input $\tau^*(t)$ is presented in Figure 4.8. The estimations of the entries of M and D matrices in (4.18) are shown in Figure 4.9. From Figure 4.2, it is seen that the tracking control objective was achieved.

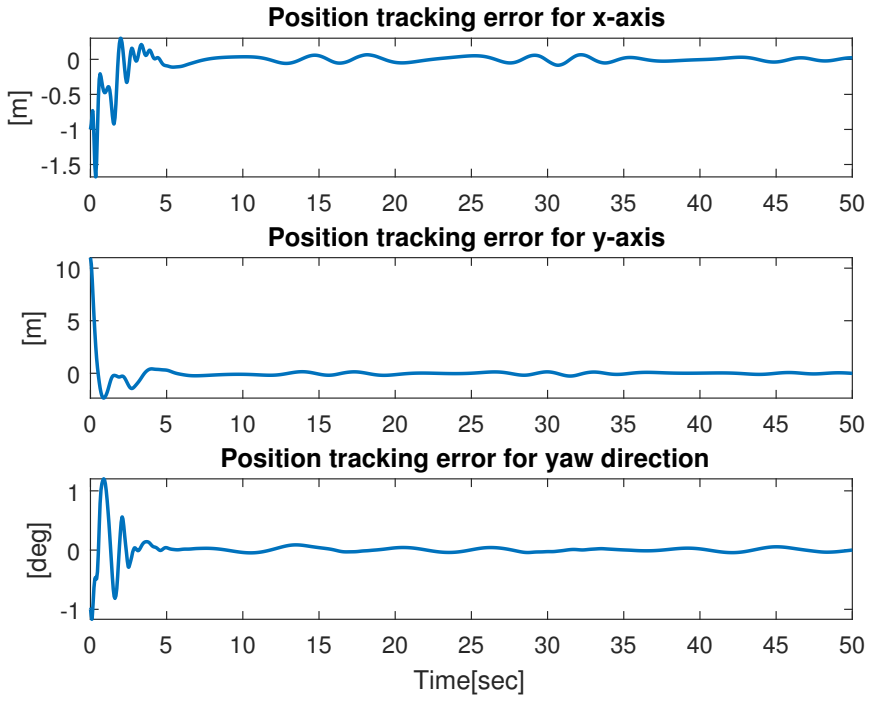

Figure 4.2. Position tracking error $e(t)$.

Additionally, for different values of harmonic limit (*i.e.*, $h = 0, 1, 3, 5$), numerical simulations were conducted. In all of these numerical simulations, the tracking control objective was met. Maximum value of $e(t)$ and $\tau^*(t)$, also $\mathcal{L}_2$ of norm of $e(t)$ were calculated and presented in Table 4.1. Based on the results given in this table, it is clearly seen that when h increases, $\mathcal{L}_2$ norm of $e(t)$ decreases.

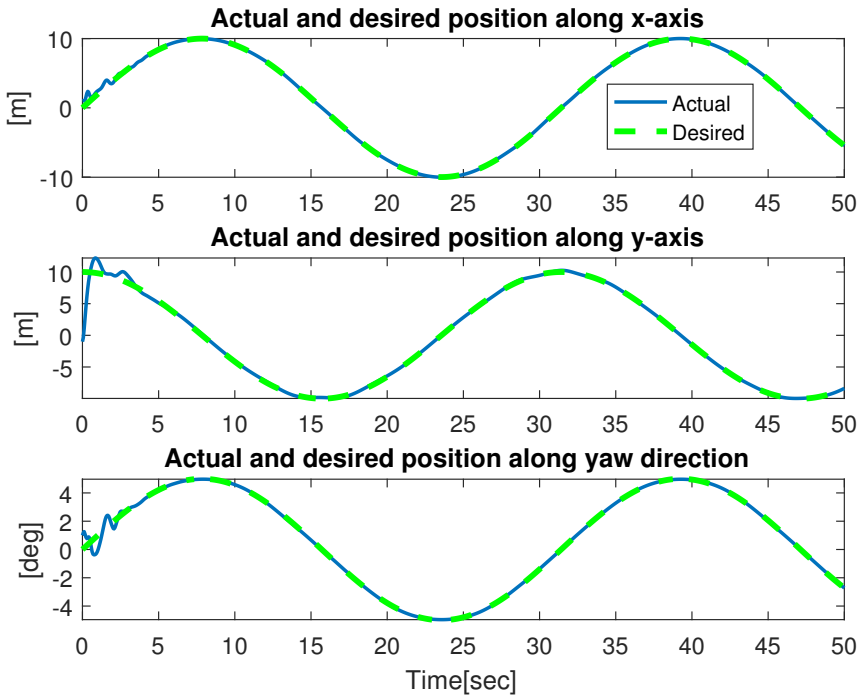

Figure 4.3. Comparison of the actual position $\eta(t)$ and the desired position $\eta_d(t)$.

4.6. Evaluation of the Method

An output feedback robust adaptive control design supported with periodic disturbance estimation was addressed for the position tracking control of unmanned surface vessels in this chapter. The lack of velocity measurements was compensated via a nonlinear velocity observer design while a Fourier series expansion like method was utilized for periodic disturbance estimation. To guarantee the convergence of the tracking error and velocity observation error under the closed–loop operation, Lyapunov based arguments were utilized. The theoretical results were supported with numerical simulations realized for the case that marine vessel was disturbed by sinusoidal perturbations in (4.82). In these simulations, it was observed that the proposed controller can be used to provide position control of marine vessels efficiently. Effect of the change of harmonic limits on the control performance was also examined and presented in a detailed manner in these simulation studies.

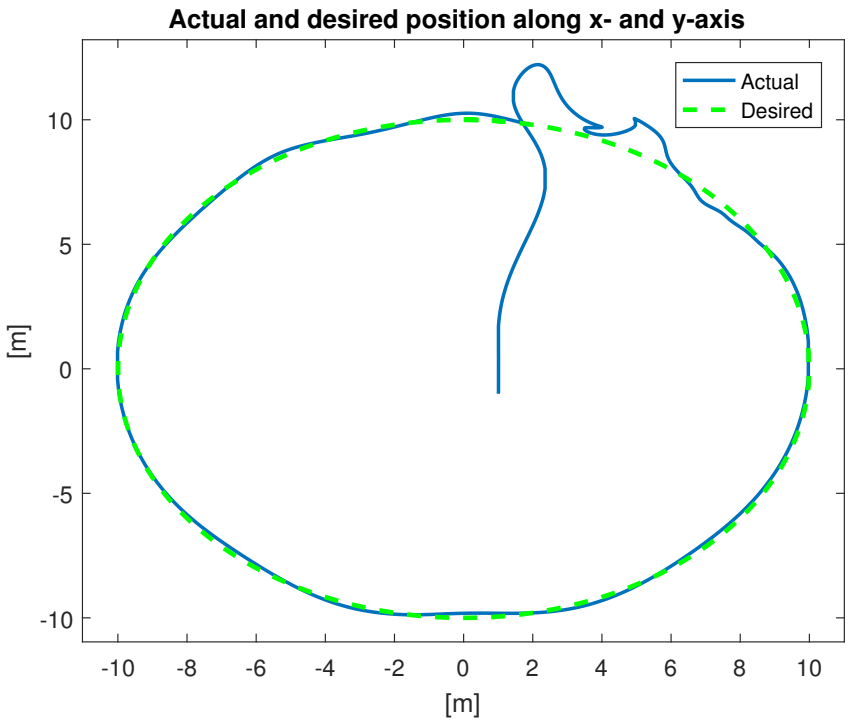

Figure 4.4. Actual position $\eta(t)$ and desired position $\eta_d(t)$ presented in xy plane.

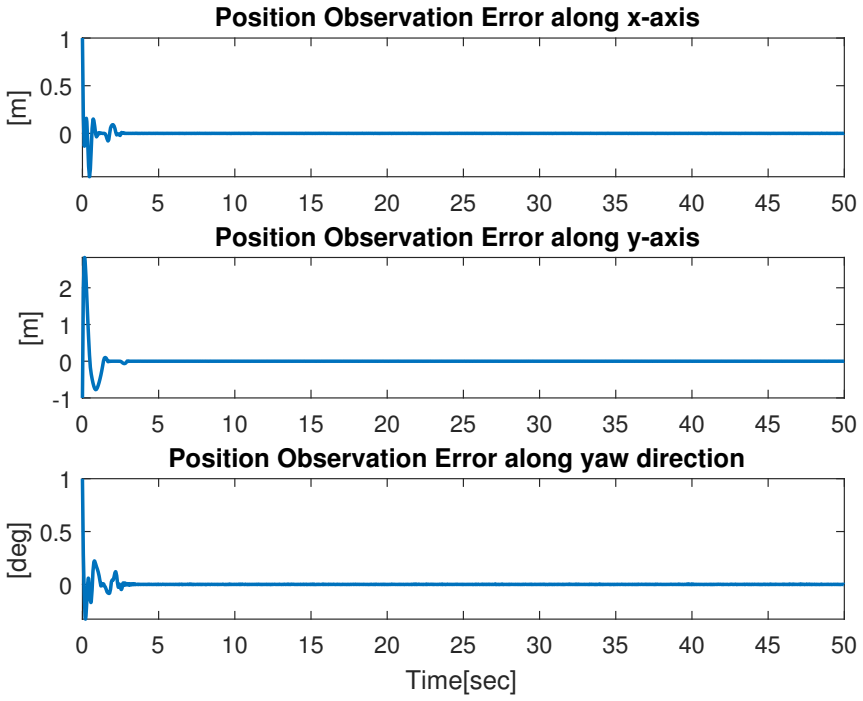

Figure 4.5. Position observation error $\tilde{\eta}(t)$.

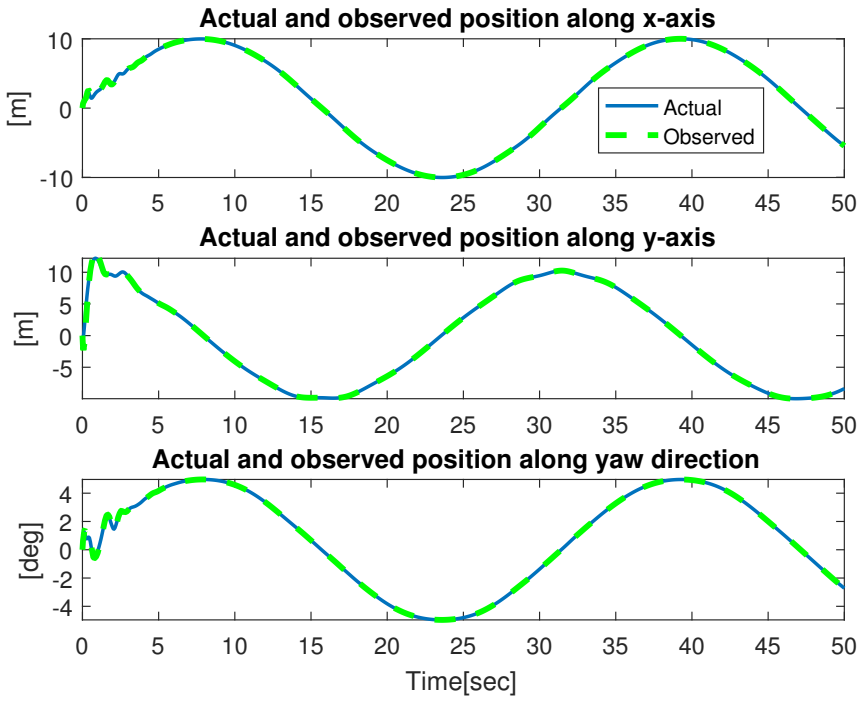

Figure 4.6. Comparison of the actual position $\eta(t)$ and the observed position $\hat{\eta}(t)$.

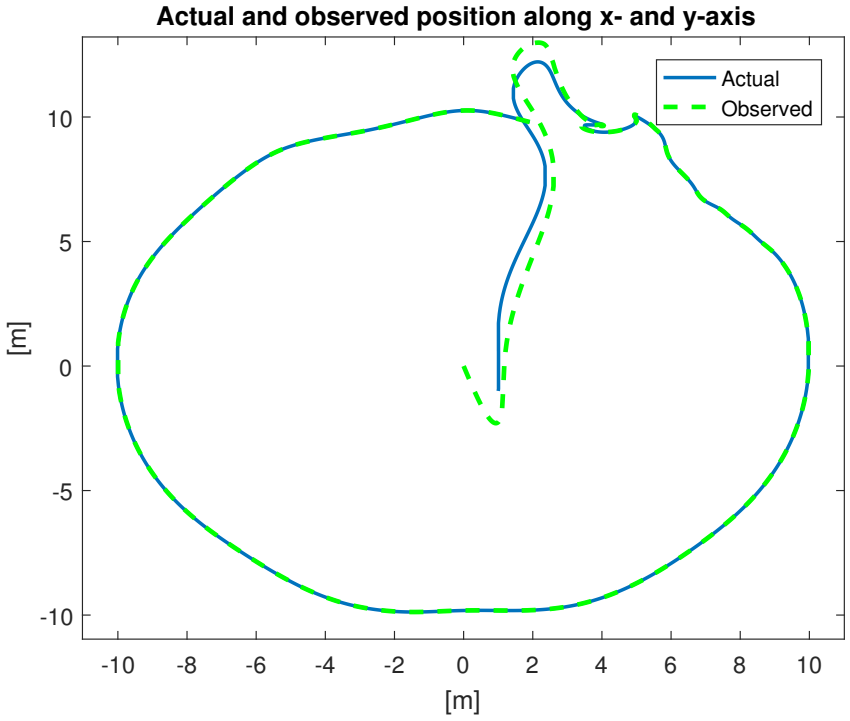

Figure 4.7. Actual position $\eta(t)$ and observed position $\hat{\eta}(t)$ presented in xy plane.

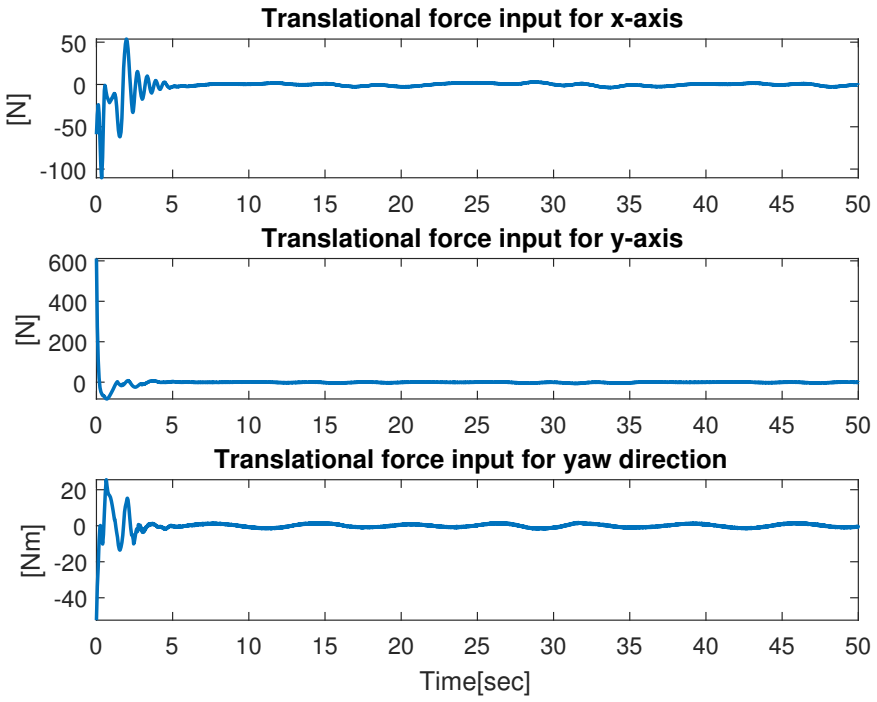

Figure 4.8. Control input torque $\tau^*(t)$.

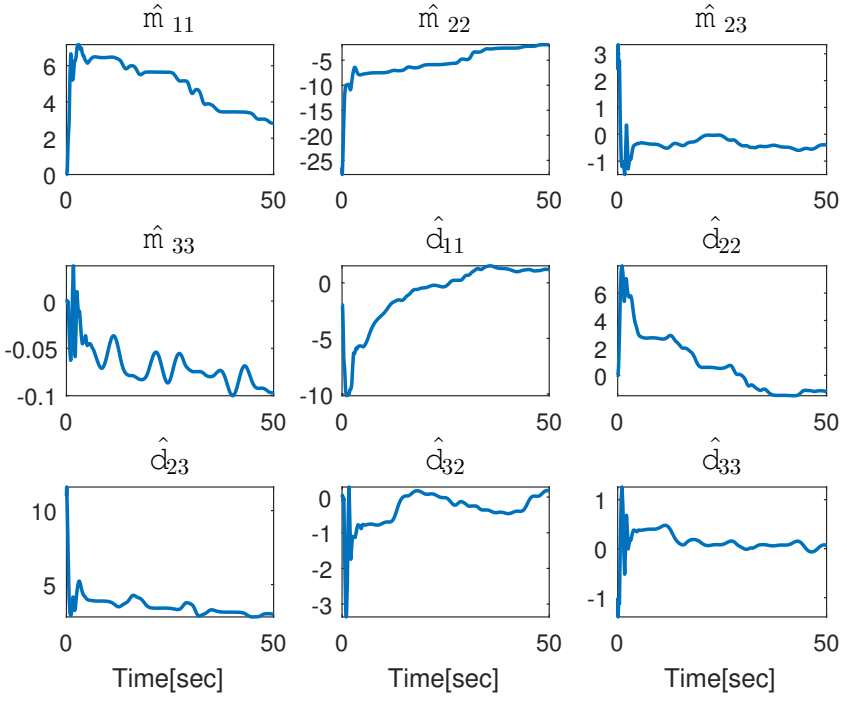

Figure 4.9. Estimations of the entries of M and D matrices.

Table 4.1. Comparison table for different harmonic limits of the approximation.

Harmonic Limit	**States**	**max value of** $e(t)$	$\mathcal{L}_2$ **norm of** $e(t)$	**max**$\lvert\tau_i^*(t)\rvert$
$h = 0$	Linear position x	0.5714	1.2114	43.2470
	Linear position y	11	5.1227	611.5837
	Yaw angle ψ	1.2420	1.2230	24.0726
$h = 1$	Linear position x	0.4878	1.1178	40.2028
	Linear position y	11	5.0303	611.5926
	Yaw angle ψ	1.2436	1.1783	26.5673
$h = 3$	Linear position x	0.3012	1.0918	53.6611
	Linear position y	11	4.9982	611.5926
	Yaw angle ψ	1.2024	1.1158	25.5485
$h = 5$	Linear position x	0.2903	0.9058	8.6887
	Linear position y	11	4.9669	611.6722
	Yaw angle ψ	1.3105	1.1144	28.1314

CHAPTER 5

CONCLUSIONS AND FUTURE WORKS

In this thesis, tracking control of marine vessels subject to model anomalies such as parametric uncertainties and additive environmental disturbances was investigated. The disturbances were considered to be periodic but its period is unknown. Two controllers were designed based on the availability of velocity feedback.

Firstly, in Chapter 3, a backstepping controller was designed for position tracking control of surface vessels when all states (*i.e.,* position and velocity) were measurable. To compensate for the unknown periodic disturbances, the method inspired from Fourier series was preferred. Stability of the closed–loop system was investigated via Lyapunov type arguments and asymptotic stability was ensured. With numerical simulation results, efficacy of the controller was presented. For different harmonic limit approximations of the series expansion, it was observed that better results were obtained for increasing harmonic limit values.

Secondly, in Chapter 4, the lack of velocity measurements in addition to the model anomalies of parametric uncertainties and environmental forces were coped with robust adaptive output feedback control design fused with the periodic disturbance estimation method. With Lyapunov type tools, asymptotic stability was proven. The theoretical results were supported with numerical simulations and it was observed that this designed controller was a good compromise between the parametric uncertainties, disturbances, and the absence of velocity measurements.

When compared with the state of the art research in control of marine vessels, the periodic disturbance estimation method is **firstly** applied for control of ships in this thesis. The closest method in the literature when dealing with the periodic disturbances is repetitive learning controllers. However, repetitive learning controllers rely on accurate knowledge of the period of the uncertainties and when the period is uncertain, which is the case examined in this thesis, they cannot be used. Another method when dealing with periodic disturbances is modeling the disturbances as the output of a dynamic linear regression model with uncertain regressor state as in Du et al. (2018). While ensuring sim-

ilar stability result (*i.e.*, asymptotic stability), that method seems to be more complicated when compared with the proposed methodology.

There are several research avenues to be considered as possible future works. In the numerical simulations, high frequency oscillations are observed in the transients of some signals. To decrease this unwanted results, as a possible extension, barrier function based control strategies can be utilized in conjunction with the proposed control algorithms. A significant amount of vessels have only a single screw propeller and a rudder as actuators (*i.e.,* control inputs), which makes them under–actuated, that is having fewer independent control inputs than the number of degrees of freedom to be controlled. Utilizing the proposed methodology in designing controllers for under–actuated ships can be a challenge to work on as an extension. Besides, the vessel motion forces the whole fluid and gives rise to oscillations with different amplitudes, which causes the inertia matrix of the vessel to lose its symmetry which aside from its practical outcomes is a theoretical issue that needs to be dealt with as symmetry of the inertia matrix is essential for the stability analysis. Therefore, taking vessels' hydro–dynamically added inertia into account can be considered as an extension. Moreover, experimental verification of the proposed controllers on a surface vessel can be an interesting future work.

REFERENCES

Agostinho, Adriana C and Moratelli Jr, Lázaro and Tannuri, Eduardo A and Morishita, Hélio Mitio (2009). Sliding mode control applied to offshore dynamic positioning systems. In *IFAC International Conference on Manoeuvring and Control of Marine Craft*, pp. 237–242.

Aksoy, Orhan and Zergeroglu, Erkan and Tatlicioglu, Enver (2017). On adaptive output feedback controf robotic manipulators with online disturbance estimation. *Journal of Intelligent & Robotic Systems 85*(3-4), 633–649.

Ang, Kiam Heong and Chong, Gregory and Li, Yun (2005). Pid control system analysis, design, and technology. *IEEE Transactions on Control Systems Technology 13*(4), 559–576.

Balchen, Jens G and Jenssen, Nils A and Mathisen, Eldar and Saelid, Steinar (1980). Dynamic positioning of floating vessles based on Kalman filtering and optimal control. In *IEEE Conference on Decision and Control*, pp. 852–864.

Balchen, Jens G and Jenssen, Nils A and Sælid, Steinar (1976). Dynamic positioning using Kalman filtering and optimal control theory. In *IFAC/IFIP Symposium on Automation in Offshore Oil Field Operation*, pp. 183–188.

Bidikli, Baris and Tatlicioglu, Enver and Zergeroglu, Erkan (2013). Observer based output feedback tracking control of dynamically positioned surface vessels. In *American Control Conference*, pp. 554–559.

Bidikli, Baris and Tatlicioglu, Enver and Zergeroglu, Erkan (2017a). Compensating of added mass terms in dynamically positioned surface vehicles: A continuous robust control approach. *Ocean Engineering 139*, 198–204.

Bidikli, Baris and Tatlicioglu, Enver and Zergeroglu, Erkan (2017b). Observer-based adaptive output feedback tracking control of dynamically positioned surface vessels.

Journal of Marine Science and Technology 22(2), 376–387.

Chen, Zheng and Zhang, Yougong and Nie, Yong and Tang, Jianzhong and Zhu, Shiqiang (2020). Adaptive sliding mode control design for nonlinear unmanned surface vessel using rbfnn and disturbance-observer. *IEEE Access 8*, 45457–45467.

Dasdemir, Janset and Zergeroglu, Erkan (2015). A new continuous high–gain controller scheme for a class of uncertain nonlinear systems. *International Journal of Robust and Nonlinear Control 25*(1), 125–141.

Delibasi, Akin and Kucukdemiral, Ibrahim B and Cansever, Galip (2006). A novel variable structure based adaptive control with disturbance estimation. In *American Control Conference*, pp. 4782–4787.

Delibasi, Akin and Zergeroglu, Erkan and Kucukdemiral, Ibrahim B and Cansever, Galip (2010). Adaptive self-tuning control of robot manipulators with periodic disturbance estimation. *International Journal of Robotics and Automation 25*(1), 48–56.

Du, Jialu and Hu, Xin and Krstić, Miroslav and Sun, Yuqing (2018). Dynamic positioning of ships with unknown parameters and disturbances. *Control Engineering Practice 76*, 22–30.

Fang, Yongchun and Zergeroglu, Erkan and De Queiroz, Marcio and Dawson, Darren M (2004). Global output feedback control of dynamically positioned surface vessels: an adaptive control approach. *Mechatronics 14*(4), 341–356.

Fjellstad, Ola-Erik and Fossen, Thor I (1994). Quaternion feedback regulation of underwater vehicles. In *IEEE Conference on Control Applications*, pp. 857–862.

Fossen, Thor I (2002). Marine control system-guidance, navigation and control of ships, rigs and underwater vehicles. *Marine Cybernetics*.

Fossen, Thor I (2011). *Handbook of marine craft hydrodynamics and motion control*. John Wiley & Sons.

Fossen, Thor I and Grovlen, Aslaug (1998). Nonlinear output feedback control of dynamically positioned ships using vectorial observer backstepping. *IEEE Transactions on Control Systems Technology 6*(1), 121–128.

Fossen, Thor I and Perez, Tristan (2009). Kalman filtering for positioning and heading control of ships and offshore rigs. *IEEE Control Systems Magazine 29*(6), 32–46.

Fossen, Thor I and Strand, Jan P (1999). Tutorial on nonlinear backstepping: Applications to ship control. *Modeling Identification and Control 20*(2), 83–135.

Fossen, Thor I and Strand, Jann Peter (1999). Passive nonlinear observer design for ships using Lyapunov methods: full-scale experiments with a supply vessel. *Automatica 35*(1), 3–16.

Fung, Patrick and Grimble, Mike (1983). Dynamic ship positioning using a self-tuning Kalman filter. *IEEE Transactions on Automatic Control 28*(3), 339–350.

Grimble, Mike J and Patton, Ron J and Wise, DA (1980). The design of dynamic ship positioning control systems using stochastic optimal control theory. *Optimal Control Applications and Methods 1*(2), 167–202.

Hassani, Vahid and Sørensen, Asgeir J and Pascoal, Antonio M and Aguiar, A Pedro (2012). Multiple model adaptive wave filtering for dynamic positioning of marine vessels. In *American Control Conference*, pp. 6222–6228.

Hu, Xin and Du, Jialu and Sun, Yuqing (2017). Robust adaptive control for dynamic positioning of ships. *IEEE Journal of Oceanic Engineering 42*(4), 826–835.

Katebi, MR and Yamamoto, Ikuo and Matsuura, Masami and Grimble, MJ and Hirayama, Hiroaki and Okamoto, Norihiko (2001). Robust dynamic ship positioning control system design and applications. *International Journal of Robust and Nonlinear Control 11*(13), 1257–1284.

Khalil, Hassan K (2002). *Nonlinear systems*. Prentice hall Upper Saddle River, NJ, USA.

Kokotovic, Petar V (1992). The joy of feedback: nonlinear and adaptive. *IEEE Control Systems Magazine 12*(3), 7–17.

Lewis, Frank L and Dawson, Darren M and Abdallah, Chaouki T (2003). *Robot manipulator control: theory and practice*. CRC Press.

Li, Zhen and Sun, Jing (2011). Disturbance compensating model predictive control with application to ship heading control. *IEEE Transactions on Control Systems Technology 20*(1), 257–265.

Liao, Yulei and Jiang, Quanquan and Du, Tingpeng and Jiang, Wen (2020). Redefined output model-free adaptive control method and unmanned surface vehicle heading control. *IEEE Journal of Oceanic Engineering*, accepted, to appear.

Loria, Antonio and Fossen, Thor I and Panteley, Elena (2000). A separation principle for dynamic positioning of ships: Theoretical and experimental results. *IEEE Transactions on Control Systems Technology 8*(2), 332–343.

Lu, Yu and Zhang, Guoqing and Qiao, Lei and Zhang, Weidong (2020). Adaptive output-feedback formation control for underactuated surface vessels. *International Journal of Control 93*(3), 400–409.

Perez, Tristan and Blanke, Mogens (2010). Ship roll motion control. In *IFAC Conference on Control Applications in Marine Systems*, pp. 1–12.

Qiao, Lei and Zhang, Weidong (2018). Adaptive second-order fast nonsingular terminal sliding mode tracking control for fully actuated autonomous underwater vehicles. *IEEE Journal of Oceanic Engineering 44*(2), 363–385.

Sørensen, Asgeir J and Sagatun, Svein I and Fossen, Thor I (1996). Design of a dynamic positioning system using model-based control. *Modeling Identification and Control 17*(2), 135–151.

Tannuri, Eduardo A and Agostinho, Adriana C (2010). Higher order sliding mode

control applied to dynamic positioning systems. In *IFAC Conference on Control Applications in Marine Systems*, pp. 132–137.

Tannuri, Eduardo A and Donha, DC and Pesce, CP (2001). Dynamic positioning of a turret moored fpso using sliding mode control. *International Journal of Robust and Nonlinear Control 11*(13), 1239–1256.

Veksler, Aleksander and Johansen, Tor Arne and Borrelli, Francesco and Realfsen, Bjørnar (2016). Dynamic positioning with model predictive control. *IEEE Transactions on Control Systems Technology 24*(4), 1340–1353.

Wang, Ning and Qian, Chunjiang and Sun, Jing-Chao and Liu, Yan-Cheng (2015). Adaptive robust finite-time trajectory tracking control of fully actuated marine surface vehicles. *IEEE Transactions on Control Systems Technology 24*(4), 1454–1462.

Wang, Ning and Sun, Zhuo and Yin, Jianchuan and Zou, Zaojian and Su, Shun-Feng (2019). Fuzzy unknown observer-based robust adaptive path following control of underactuated surface vehicles subject to multiple unknowns. *Ocean Engineering 176*, 57–64.

Wondergem, Michiel and Lefeber, Erjen and Pettersen, Kristin Y and Nijmeijer, Henk (2010). Output feedback tracking of ships. *IEEE Transactions on Control Systems Technology 19*(2), 442–448.

Xian, Bin and Dawson, Darren M and de Queiroz, Marcio S and Chen, Jian (2004). A continuous asymptotic tracking control strategy for uncertain nonlinear systems. *IEEE Transactions on Automatic Control 49*(7), 1206–1211.

Yunsheng, Fan and Xiaojie, Sun and Guofeng, Wang and Chen, Guo (2015). On fuzzy self-adaptive pid control for usv course. In *Chinese Control Conference*, pp. 8472–8478.

Zergeroglu, Erkan and Tatlicioglu, Enver and Kaleli, Egemen (2017). A model

independent observer based output feedback tracking controller for robotic manipulators with dynamical uncertainties. *Robotica 35*(4), 729–743.

Zhang, Jun and Sun, Tairen and Liu, Zhilin (2017). Robust model predictive control for path-following of underactuated surface vessels with roll constraints. *Ocean Engineering 143*, 125–132.

Zhu, Guibing and Du, Jialu (2018). Global robust adaptive trajectory tracking control for surface ships under input saturation. *IEEE Journal of Oceanic Engineering 45*(2), 442–450.

APPENDIX A

PROOFS OF BOUNDS

In this appendix, the proofs of upper bounds in (3.35), (4.45) and (4.54) are given (Dasdemir and Zergeroglu, 2015).

A.1. Proof of Bound in (3.35)

Substituting (3.5) and (3.17) into (3.34) yields

$$\begin{aligned}\chi &= MR^T(\psi_d)\ddot{\eta}_d - MR^T(\psi_d)\dot{R}(\psi_d)R^T(\psi_d)\dot{\eta}_d + DR^T(\psi_d)\dot{\eta}_d \\ &\quad -D\nu + MSR^T(\psi)\dot{\eta}_d - MS(\dot{\psi})R^T(\psi)K_1z_1 - MR^T(\psi)\ddot{\eta}_d \\ &\quad +MR^T(\psi)K_1R(\psi)\nu - MR^T(\psi)K_1\dot{\eta}_d. \end{aligned} \tag{A.1}$$

In the view of the property of rotational matrix which is $\dot{R}(\psi_d) = R(\psi_d)S(\dot{\psi}_d)$ and making use of (3.1) and (3.9), following expressions can be obtained

$$\begin{aligned}\chi &= M[R^T(\psi_d) - R^T(\psi)]\ddot{\eta}_d + M[S(\dot{\psi})R^T(\psi) - S(\dot{\psi}_d)R^T(\psi_d)]\dot{\eta}_d \\ &\quad +D[R^T(\psi_d)\dot{\eta}_d - R^T(\psi)\dot{\eta}] - MS(\dot{\psi})R^T(\psi)K_1z_1 \\ &\quad +MR^T(\psi)K_1(\dot{\eta} - \dot{\eta}_d) \\ &= M[R^T(\psi_d) - R^T(\psi)]\ddot{\eta}_d + M[S(\dot{\psi})R^T(\psi) - S(\dot{\psi}_d)R^T(\psi) \\ &\quad +S(\dot{\psi}_d)R^T(\psi) - S(\dot{\psi}_d)R^T(\psi_d)]\dot{\eta}_d + D[R^T(\psi_d)\dot{\eta}_d \\ &\quad -R^T(\psi)\dot{\eta}_d + R^T(\psi)\dot{\eta}_d - R^T(\psi)\dot{\eta}] - MS(\dot{\psi})R^T(\psi)K_1z_1 \\ &\quad +MR^T(\psi)K_1(K_1z_1 - Rz_2) \\ &= M[R^T(\psi_d) - R^T(\psi)]\ddot{\eta}_d + M[S(\dot{\psi}) - S(\dot{\psi}_d)]R^T(\psi)\dot{\eta}_d \\ &\quad +MS(\dot{\psi}_d)[R^T(\psi) - R^T(\psi_d)]\dot{\eta}_d + D[R^T(\psi_d) - R^T(\psi)]\dot{\eta}_d \\ &\quad +DR^T(\psi)(K_1z_1 - R(\psi)z_2) - MS(\dot{\psi})R^T(\psi)K_1z_1 \\ &\quad +MR^T(\psi)K_1(K_1z_1 - R(\psi)z_2). \end{aligned} \tag{A.2}$$

The dynamics terms M, D and kinematic terms $R(\psi)$, $S(\dot{\psi})$ have the following upper bounds

$$\begin{aligned}
\left\|R(\psi_d) - R(\psi)\right\|_{i\infty} &\leq \xi_{R1}\|z_1\| && \text{(A.3)}\\
\left\|S(\dot{\psi}) - S(\dot{\psi}_d)\right\|_{i\infty} &\leq \xi_{S1}\|\dot{z}_1\| \leq \xi_{S1}(\lambda_{\max}(K_1)\|z_1\| + \|z_2\|) && \text{(A.4)}\\
\left\|S(\dot{\psi}_d)\right\|_{i\infty} &\leq \xi_{S2} && \text{(A.5)}\\
\|D\|_{i\infty} &\leq \lambda_{\max}(D) && \text{(A.6)}\\
\|M\|_{i\infty} &\leq \lambda_{\max}(M) && \text{(A.7)}\\
\|\dot{\eta}_d\| &\leq \xi_{\eta 1} && \text{(A.8)}\\
\|\ddot{\eta}_d\| &\leq \xi_{\eta 2} && \text{(A.9)}\\
\left\|S(\dot{\psi})\right\|_{i\infty} \leq \left\|\dot{\psi}\right\| \leq \|\dot{\eta}\| &\leq \|\dot{\eta}_d\| + \|\dot{z}_1\| \leq \|\dot{\eta}_d\| + \lambda_{\max}(K_1)\|z_1\| + \|z_2\| && \text{(A.10)}
\end{aligned}$$

where $\xi_{R1}, \xi_{S1}, \xi_{S2}, \xi_{\eta 1}, \xi_{\eta 2} \in \mathbb{R}$ are positive constants and $\left\|(\cdot)\right\|_{i\infty}$ is the induced infinity norm.

After utilizing the given upper bound properties of dynamic and kinematic terms, the right hand side of (A.2) can be upper bounded as

$$\begin{aligned}
\|\chi\| \leq\ & \lambda_{\max}(M)\xi_{R1}\xi_{\eta 2}\|z_1\| + \lambda_{\max}(M)\lambda^2_{\max}(K_1)\|z_1\| \\
& + \lambda_{\max}(M)\xi_{S1}\xi_{\eta 1}\left[\ \lambda_{\max}(K_1)\|z_1\| + \|z_2\|\ \right] + \lambda_{\max}(M)\xi_{S2}\xi_{R1}\xi_{\eta 1}\|z_1\| \\
& + \lambda_{\max}(D)\xi_{R1}\xi_{\eta 1}\|z_1\| + \lambda_{\max}(D)\lambda_{\max}(K_1)\|z_1\| \\
& + \lambda_{\max}(M)\lambda_{\max}(K_1)\|z_2\| + \lambda_{\max}(D)\|z_2\| \\
& + \lambda_{\max}(M)\lambda_{\max}(K_1)\|z_1\|\left[\ \xi_{\eta 1} + \lambda_{\max}(K_1)\|z_1\| + \|z_2\|\ \right]. \qquad \text{(A.11)}
\end{aligned}$$

To obtain a compact form of the above equation, terms c_1, c_2, c_3 and c_4 can be defined as

$$\begin{aligned}
c_1 \triangleq\ & \lambda_{\max}(M)\xi_{R1}\xi_{\eta 2} + \lambda_{\max}(M)\lambda^2_{\max}(K_1) + \lambda_{\max}(M)\xi_{S1}\xi_{\eta 1}\lambda_{\max}(K_1) \\
& + \lambda_{\max}(M)\xi_{S2}\xi_{R1}\xi_{\eta 1} + \lambda_{\max}(D)\xi_{R1}\xi_{\eta 1} + \lambda_{\max}(D)\lambda_{\max}(K_1) \\
& + \lambda_{\max}(M)\xi_{\eta 1}\lambda_{\max}(K_1) && \text{(A.12)}\\
c_2 \triangleq\ & \lambda_{\max}(M)\lambda_{\max}(K_1) + \lambda_{\max}(D) + \lambda_{\max}(M)\xi_{S1}\xi_{\eta 1} && \text{(A.13)}
\end{aligned}$$

$$c_3 \triangleq \lambda_{\max}(M)\lambda^2_{\max}(K_1) \tag{A.14}$$

$$c_4 \triangleq \lambda_{\max}(M)\lambda_{\max}(K_1) \tag{A.15}$$

thus the bound given in (3.35) is achieved.

A.2. Proof of Bound in (4.45)

In view of the Properties 1, 3 and 4, substituting (4.39) and (4.19) into (4.44) yields

$$\begin{aligned}\|\chi\| \leq\ & \{\alpha^2 m_u + \zeta_{j1}\|\ddot{\eta}_d\| + 2\alpha\zeta_{c1}\|\dot{\eta}_d\| + \zeta_{f2}\|\dot{\eta}_d\| + \alpha\zeta_{f1} + \zeta_{c2}\|\dot{\eta}_d\|^2 \\ & +\alpha^2\zeta_{c1}\|e\|\}\|e\| + \{\alpha m_u + \zeta_{c1}\|\dot{\eta}_d\| + \alpha\zeta_{c1}\|e\|\}\|r\|\end{aligned} \tag{A.16}$$

Selection of the bounding functions $\rho_1(e)$ and $\rho_2(e)$ as

$$\begin{aligned}\rho_1(e) \triangleq\ & \alpha^2 m_u + \zeta_{j1}\|\ddot{\eta}_d\| + 2\alpha\zeta_{c1}\|\dot{\eta}_d\| + \zeta_{f2}\|\dot{\eta}_d\| + \alpha\zeta_{f1} + \zeta_{c2}\|\dot{\eta}_d\|^2 \\ & +\alpha^2\zeta_{c1}\|e\|\end{aligned} \tag{A.17}$$

$$\rho_2(e) \triangleq \alpha m_u + \zeta_{c1}\|\dot{\eta}_d\| + \alpha\zeta_{c1}\|e\| \tag{A.18}$$

satisfies the bound in (4.45).

A.3. Proof of Bound in (4.54)

After utilizing the Properties 1, 3 and 4 along with (4.53), we can reach

$$\begin{aligned}\|N_b\| \leq\ & \frac{1}{m_l}\{\zeta_{j2} m_u m_l\|\ddot{\eta}_d\| + \zeta_{j2} m_l\left\|Y_d\tilde{\theta}\right\| + \zeta_{c2}\|\dot{\eta}_d\|^2 + \zeta_{f2}\|\dot{\eta}_d\| \\ & +K_{p,\max}\}\|e\| + \frac{1}{m_l}2\zeta_{c1}\|\dot{\eta}_d\| + \zeta_{f1} + K_{c,\max}\|r\| + \frac{\zeta_{c2}\|\dot{\eta}_d\|}{m_l}\|e\|\|r\| \\ & +\frac{\zeta_{c1}}{m_l}\|r\|^2 + \frac{K_{c,\max}}{m_l}\|s\|\end{aligned} \tag{A.19}$$

where $\|\dot{e}\| \leq \|r\|$ was utilized (Lewis et al., 2003). Bounding constants $\rho_{0i}, i = 1, .., 5$ can be defined in view of (A.19)

$$\begin{aligned}
\rho_{01} &\triangleq \frac{1}{m_l}\{\zeta_{j2} m_u m_l \|\ddot{\eta}_d\| + \zeta_{j2} m_l \left\|Y_d \tilde{\theta}\right\| + \zeta_{c2}\|\dot{\eta}_d\|^2 + \zeta_{f2}\|\dot{\eta}_d\| \\
&\quad + K_{p,\max}\} && \text{(A.20)} \\
\rho_{02} &\triangleq \frac{1}{m_l}\{2\zeta_{c1}\|\dot{\eta}_d\| + \zeta_{f1} + K_{c,\max}\} && \text{(A.21)} \\
\rho_{03} &\triangleq \frac{\zeta_{c2}\|\dot{\eta}_d\|}{m_l} && \text{(A.22)} \\
\rho_{04} &\triangleq \frac{\zeta_{c1}}{m_l} && \text{(A.23)} \\
\rho_{05} &\triangleq \frac{K_{c,\max}}{m_l}. && \text{(A.24)}
\end{aligned}$$

Hence, the upper bound of $\|N_b\|$ in (4.54) is obtained.